3 Group VII Transition Metal Carbene Cluster Complexes

3.1 Introduction

3.1.1 Background

Carbene chemistry of transition metals such as chromium and tungsten is well developed and known routes exist to control and manipulate this chemistry.[1] For transition metals such as manganese and cobalt, discoveries made are still often serendipitous.

Fischer's method of *in situ* preparation of metal carbonyl carbene complexes is most successful with the Group VI transition metal carbonyl complexes.[2] However, on going from the d^6 to the d^8 transition metals, Fischer[3] and others[4] have had difficulty alkylating analogous iron acylates of the form $[Fe(CO)_4C(O)OR]^-$. Attempted methylation of $[Fe(CO)_4C(O)Ph]^-Li^+$ with $Me_3O^+BF_4^-$ lead to formation of $Fe_3(CO)_{12}$ and $Fe_2(CO)_9$ as the major reaction products. Alkylation of iron tetracarbonyl acylates by $Et_3O^+BF_4^-$ was observed

[1] Sierra, M.A. *Chem. Rev.* **2000**, *100*, 3591.
[2] Aumann, R.; Fischer, E.O. *Angew. Chem., Int. Ed. Engl.* **1967**, *6*, 878.
[3] Fischer, E.O.; Kiene, V. *J. Organomet. Chem.* **1970**, *23*, 215.
[4] (a) Collman, J.P. *Acc. Chem. Res.* **1975**, *8*, 342, (b) Petz, W. *Organometallics* **1983**, *2*, 1044, (c) Jiabi, C.; Guixin, L.; Weihua, X.; Xianglin, J.; Meicheng, S.; Yougi, T. *J. Organomet. Chem.* **1985**, *286*, 55, (d) Semmelhack, M.F.; Tamura, R. *J. Am. Chem. Soc.* **1983**, *105*, 4099, (e) Lotz, S.; van Rooyen, P.H.; van Dyk, M.M. *Organometallics* **1987**, *6*, 499.

only when R was a very electron withdrawing group, such as C_6F_5 or C_6Cl_5.[5] However, for complexes of the form $[FeL(CO)_3C(O)R]^-Li^+$ (L = PR_3 or $P(OR)_3$) alkylation with oxonium salts readily yields the corresponding carbene complexes $[FeL(CO)_3C(OEt)R]$.[6] The yield of the carbene complexes was found to be dependent on the electronic character of the ligand L; the less electron donating ligands promoting higher yields.

In the case of the tetracarbonyl iron acylate, metal alkylation instead of *O*-alkylation has been ascribed to the fact that these $[Fe(CO)_4C(O)OR]^-$ anions are basic, and have two possible coordination sites for Lewis acids: one at the metal and the other at the alkoxy carbonyl or the carbamoyl oxygen atom.[4(b)] In contrast, the corresponding Group VI anions $[Cr(CO)_5C(O)OR]^-$ have only one site because two electrons at the metal are replaced by a CO group to achieve noble gas configuration. Attack of an electrophile at the metal centre is therefore not expected.

An intermediate situation is expected for d^7 transition metal acylate anions. Due to the uneven number of valence electrons of Group VII transition metals, complexes of these metals require at least one X-type ligand, as classified by Green.[7] In the case of dimanganese or dirhenium nonacarbonyl carbene complexes, this implies that the $M(CO)_5$-moiety is the X-type ligand present, or in the case of η^5-cyclopentadienyl manganese dicarbonyl carbene complex, the Cp ligand constitutes an L_2X-type ligand. Compared to Group VI transition metal carbonyl complexes, more reactive intermediates are therefore possible when Group VII transition metal complexes react with nucleophiles due to the presence of both L- and X-type ligands in the precursors.

[5] Fischer, E.O.; Beck, H.J.; Kreiter, C.G.; Lynch, J.; Müller, J.; Winkler, E. *Chem. Ber.* **1972**, *105*, 162.
[6] Conder, H.L.; York Darensbourg, M. *Inorg. Chem.* **1974**, *13*, 3.
[7] Green, M.L.H. *J. Organomet. Chem.* **1995**, *500*, 127.

3.1.2 Monomanganese carbene complexes

The King compound [Mn$_2$(CO)$_9$(COCH$_2$CH$_2$CH$_2$)], which was initially assigned an incorrect structure without a carbene ligand [Mn$_2$(CO)$_{10}$(CH$_2$)$_3$],[8] sparked interest in the challenges associated with the synthesis of [M(CO)$_4$(carbene)X] (M = Mn, Re; X = halogen) complexes (Figure 3.1). Casey later employed proton NMR spectroscopy to assign the correct structure.
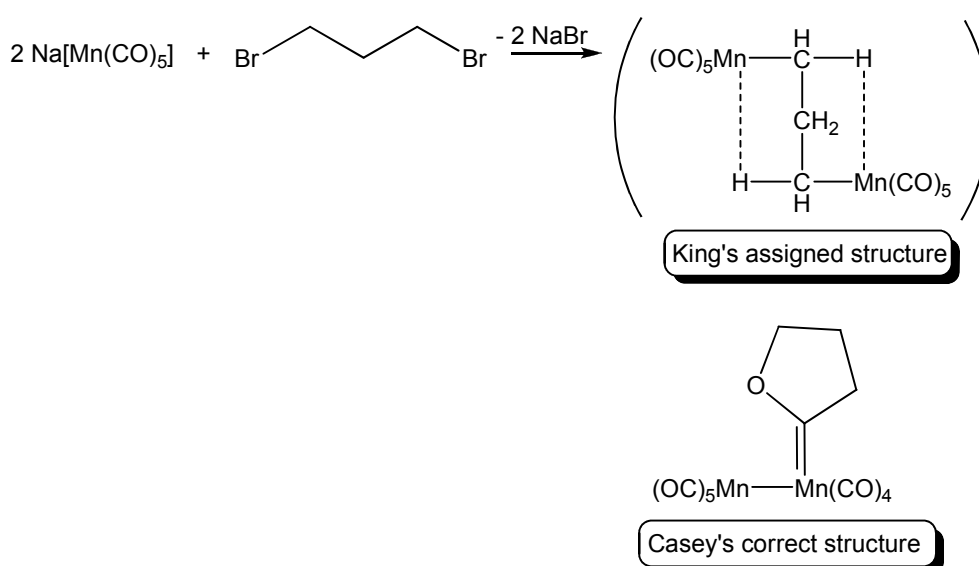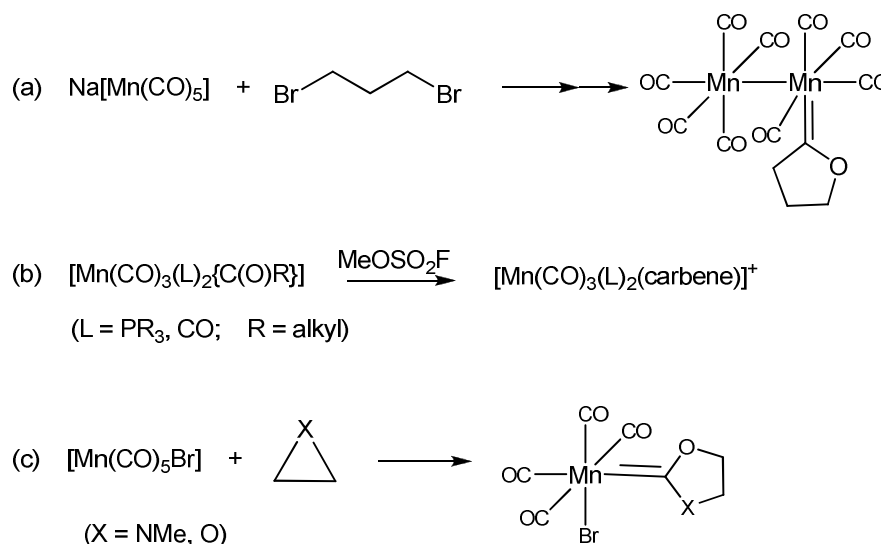

Figure 3.1   First synthesis of a manganese carbene complex

The isolation of binuclear monocarbene complexes of Group VII transition metals, [Mn$_2$(CO)$_9${C(OR)R}], (R = alkyl) prepared from Na[Mn(CO)$_5$] and 1,3-dihaloalkanes was reinvestigated and resulted in detailed mechanistic studies of the reactions of Na[M(CO)$_5$] (M = Mn, Re) with dihaloalkanes being undertaken.[9] By using different dihaloalkanes, a number of complexes similar to the King compound all containing a cyclic carbene ligand were synthesized and

---

[8] King, R.B. *J. Am. Chem. Soc.* **1963**, *85*, 1922.

[9] (a) Casey, C.P. *J. Chem. Soc., Chem. Commun.* **1970**, 1220, (b) Casey, C.P.; Cyr, C.R.; Anderson, R.L.; Marten, D.F.; *J. Am. Chem. Soc.* **1975**, *97*, 3053, (c) Casey, C.P.; Anderson, R.L. *J. Am. Chem. Soc.* **1971**, *93,* 3554, (d) Casey, C.P.; Cyr, C.R. *J. Organomet. Chem.* **1973**, *37*, C69.

characterized (Scheme 3.1 (a)).[10] In a few instances, with more sophisticated chloro precursors, cationic mononuclear carbene complexes $[Mn(CO)_3(L)_2(carbene)]^+$ (L = phosphine or CO) could be obtained, which after subsequent treatment with halides, afforded the desired neutral halo-carbene complexes $[M(CO)_4(carbene)X]$.[11]

(a) $Na[Mn(CO)_5]$ +   Br⌒⌒Br   →

(b) $[Mn(CO)_3(L)_2\{C(O)R\}]$ $\xrightarrow{MeOSO_2F}$ $[Mn(CO)_3(L)_2(carbene)]^+$

(L = PR_3, CO;   R = alkyl)

(c) $[Mn(CO)_5Br]$ +   △   →

(X = NMe, O)

Scheme 3.1

However, the complexes $[Mn(CO)_3(L)_2(carbene)]^+$ (L = PR_3 or CO) could be prepared by employing the alkylation of $[Mn(CO)_3(L)_2\{C(O)R\}]$ with the strong alkylating agent $MeOSO_2F$[12] (Scheme 3.1, (b)). Another major contribution to the carbene chemistry of Group VII transition metals came from the group of Angelici[13] with the reaction of strained 3-membered heterocyclic substrates with $M(CO)_5X$ (M = Mn, Re; X = Br, Cl). The reactions of aziridine and oxirane with

[10] (a) Garner, J.-A.M.; Irving, A.; Moss, J.R. *Organometallics,* **1990***, 9,* 2836, (b) Anderson, J.-A.M.; Archer, S.J.; Moss, J.R.; Niven, M.L. *Inorg. Chim. Acta,* **1993**, *206*, 187.

[11] (a) Fraser, P.J.; Roper, W.R.; Stone, F.G.A. *J. Chem. Soc., Dalton Trans.* **1974**, 760, (b) Game, C.H.; Green, M.; Stone, F.G.A. *J. Chem. Soc., Dalton Trans.* **1975**, 2280, (c) Green, M.; Moss, J.R.; Nowell, I.W.; Stone, F.G.A. *J. Chem. Soc., Chem. Commun.* **1972**, 1339, (d) Game, C.H.; Green, M.; Moss, J.R.; Stone, F.G.A. *J. Chem. Soc., Dalton Trans.* **1974**, 351, (e) Bowen, D.H.; Green, M.; Grove, D.M.; Moss, J.R.; Stone, F.G.A. *J. Chem. Soc., Dalton Trans.* **1974**, 1189, (f) Hartshorn, A.J.; Lappert, M.F.; Turner, K. *J. Chem. Soc., Dalton Trans.* **1978**, 348.

[12] Treichel, P.M.; Wagner, K.P. *J. Organomet. Chem.* **1975***, 88*, 199.

[13] (a) Singh, M.M.; Angelici, R.J. *Inorg. Chim. Acta* **1985**, *100*, 57, (b) Miessler, G.L.; Kim, S.; Jacobson, R.A.; Angelici, R.J. *Inorg. Chem.* **1984**, *23*, 2699, (c) Singh, M.M.; Angelici, R.J. *Inorg. Chem.* **1987**, *26* 1690.

these reagents afforded 5-membered cyclic aminooxy- and dioxycarbene compounds (Scheme 3.1 (c)). The reaction could also be applied to $M_2(CO)_{10}$ (M = Mn, Re). Largely unnoticed in later work, the cleavage of the metal-metal bond of the dioxycarbene complexes by bromine was also reported.[13(a)] Nevertheless, very few examples exists where the ligand in $[M(CO)_4(carbene)X]$ (M = Mn, Re; X = halogen) is not a cyclic alkoxycarbene.

This prompted the synthesis of dimanganese monocarbene complexes $[Mn_2(CO)_9\{C(OEt)(heteroaryl)\}]$ in our laboratories following the classical Fischer method, and a range of complexes containing heteroaromatic substituents, e.g. 2,2'-bithiophene, thiophene, furan and N-methyl pyrrole, was isolated.[14] The oxidative cleaving of the metal-metal bonds in these complexes (Scheme 3.2) with halogens yielded the corresponding monometal carbene complexes.
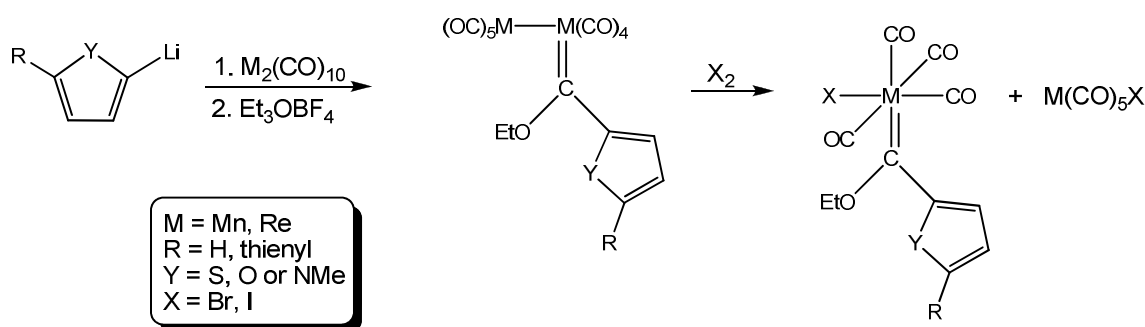
Scheme 3.2

3.1.3 π-arene substituted carbene complexes

When the structures of the Group VI complexes $[Cr(CO)_5\{C(OMe)Ph\}]$[15] and $[Cr(\eta^6\text{-}C_6H_6)(CO)_2\{C(OMe)Ph\}]$[16] (in which the carbene ligand was kept constant) were compared, it was found that increased metal-C(carbene) backbonding

---

[14] Lotz, S.; Landman, M.; Bezuidenhout, D.I.; Olivier, A.J.; Liles, D.C.; van Rooyen, P.H. *J. Organomet. Chem.* **2005**, *690*, 5929.

[15] Mills, O.S.; Redhouse, A.D. *J. Chem. Soc. (A)* **1968**, 642.

[16] Schubert, U. *J. Organomet. Chem.* **1980**, *185*, 373.

occurred for the π-arene complex. A shorter Cr-C(carbene) distance (1.935(12) Å *vs* 2.04(3) Å), and a longer C(carbene)-O distance (1.364(15) Å *vs* 1.33(2) Å) was observed for the η^6-benzene substituted complex. The observation is ascribed to the electronic nature of the π-arene ligand: these ligands induce the metal complex fragments to become better π-donors compared to the analogous $(CO)_nM$-fragments.[17] If the metal complex fragment becomes a stronger competitor for π-bonding with the carbene carbon, then the influence of the methoxy group is reduced.

A wide variety of carbene complexes has been prepared and structurally characterized in which π-bonded aromatic moieties, mainly the η^5-cyclopentadienyl (Cp) or η^5-methylcyclopentadienyl (MeCp) groups, are present as co-ligands. The first monomanganese complex of this nature to be prepared was the complex $[MnCp(CO)_2\{C(OMe)Ph\}]$.[18] After addition of PhLi to $[CpMn(CO)_3]$, the resultant acylate was protonated with a mineral acid such as H_2SO_4 and methylated with CH_2N_2 in ether.

The structural characterization[19] of $[MnCp(CO)_2\{C(OEt)Ph\}]$ revealed that, here too, the π-aromatic ligand produces efficient metal-C(carbene) back bonding. A practical consequence of this bonding situation is the presence of high Mn-C bond order. No π-donating organic substituent at the carbene carbon is therefore necessary to obtain stable complexes. Another consequence is that the presence of an oxy-substituent does not influence the Mn-C(carbene) distances significantly. The same bond lengths (1.87 – 1.89 Å) have been observed in $[MnCp(CO)_2\{C(X)Y\}]$ whether X or Y is bonded to the carbene carbon *via* an oxygen atom, or both X and Y are bonded *via* carbon atoms.

However, constant bond lengths can only be expected as long as none of the organic substituents competes effectively with the metal complex fragment. The distinct lengthening of the Mn-C(carbene) distances in the ylide-substituted

---

[17] Dötz, K.H.; Fischer, H.; Hofmann, P.; Kreissl, F.R.; Schubert, U.; Weiss, K. *Transition Metal Carbene Complexes,* VCH Verlag Chemie, Weinheim, **1983**.
[18] (a) Fischer, E.O.; Öffhaus, E.; *Chem. Ber.* **1967**, *100*, 2445, (b) Fischer, E.O.; Öffhaus, E.; Müller, J.; Nothe, D. *Chem. Ber.* **1972**, *105*, 3027.
[19] Schubert, U. *Organometallics* **1982***, 1*, 1085.

complexes [MnMeCp(CO)$_2${C(OMe)C(Me)PMe$_3$}][20] (1.99(1) Å) and [MnCp(CO)$_2$ {C(CO$_2$Me)CHPPh$_3$}][21] (1.985(3) Å) indicated that in these complexes, the organic substituents are better π-donors than the Mn(MeCp)(CO)$_2$-fragment.

Following the synthesis of heterodimetallic Group VI carbene complexes by the addition of ferrocenyl lithium (FcLi) to M(CO)$_6$ (M = Cr, W) and alkylation with either Me$_3$OBF$_4$ or Et$_3$OBF$_4$,[22] the preparation of the complexes [CpV(CO)$_3${C(OR)Fc}] and [CpCo(CO){C(OR)Fc}] in the same manner was attempted. This proved unsuccessful, and in each case, only unreacted starting material and ferrocene were recovered. Repeating the reaction with (CpMe)Mn(CO)$_3$ yielded the desired product [(MeCp)Mn(CO)$_2${C(OMe)Fc}] as the first example of a ferrocenyl CpMn-carbene complex.

3.1.4 Dirhenium carbene complexes

To determine whether binuclear metal carbonyl complexes can accommodate carbene ligands, Fischer and Öffhaus[23] successfully synthesized the binuclear [M$_2$(CO)$_9${C(OR')R}] complexes (M = Mn, Tc, Re; R = alkyl or aryl; R' = alkyl). Following the first paper reporting the preparation of the alkoxycarbene complexes [Mn$_2$(CO)$_9${C(OEt)Me}] and [Mn$_2$(CO)$_9${C(OEt)Ph}], there was some uncertainty as to whether the carbene ligand was in an equatorial or axial position. From the IR spectrum, nine carbonyl stretching bands were observed for [Mn$_2$(CO)$_9${C(OEt)Me}], corresponding to the C_s symmetry of an equatorial [Mn$_2$(CO)$_9$L] complex. However, for [Mn$_2$(CO)$_9${C(OEt)Ph}], five v$_{CO}$ bands, corresponding to C_{4v} symmetry of an axial [Mn$_2$(CO)$_9$L] complex were seen in the IR spectrum. Shortly after this, Huttner and Regler[24] reported the crystal structure of [Mn$_2$(CO)$_9${C(OEt)Ph}] and found the carbene ligand to be in an equatorial position, with the ethyl group in the *syn* configuration with respect to

[20] (a) Malisch, W.; Blau, H.; Schubert, U.; *Angew. Chem.* **1980**, *92*, 1065, (b) Malisch, W.; Blau, H.; Schubert, U. *Chem. Ber.* **1983**, *116*, 690.
[21] Kolobova, N.E.; Ivanov, L.L.; Zhvanko, O.S.; Chechulina, I.N.; Batsanov, A.S.; Struchkov, Y.T. *J. Organomet. Chem.* **1982**, *238*, 223.
[22] Connor, J.A.; Lloyd, J.P. *J. Chem. Soc., Dalton Trans.* **1972**, 1470.
[23] Fischer, E.O.; Öffhaus, E.; *Chem. Ber.* **1969**, *102*, 2449.
[24] Huttner, G.; Regler, D. *Chem. Ber.* **1972**, *105,* 1230.

the phenyl group about the C-O bond, in contrast to the *anti* configuration found in the X-ray crystal structure of $[Cr(CO)_5\{C(OMe)Ph\}]$.[24]

This result was ascribed to the fact that an equatorial carbene ligand would be too sterically hindered to accommodate the substituents on the carbene ligand in the *anti* configuration, and they explained the appearance of five IR bands instead of nine as the result of degeneracy and band overlap.
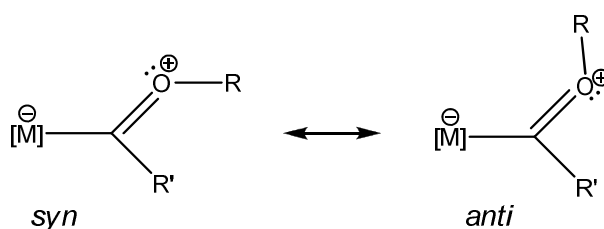
Figure 3.2   *Syn-* and *anti* configurations around the C-O bond

### 3.1.5   Axial or equatorial carbene ligands of nonacarbonyl dimetal complexes

For complexes of the type $[M_2(CO)_9(carbene)]$ (M = Mn, Tc, Re), the preferred substitution site for the carbene ligand is the electronically favoured equatorial position, where the weaker π-acceptor carbene ligand lies *trans* to a stronger π-acid carbonyl, rather than *trans* to the X-ligand, the $M(CO)_5$-moiety.

However, it was found that for dimetal nonacarbonyl carbene complexes, the site for carbene substitution can be manipulated by the steric bulk of the carbene ligand substituents.[25] During the aminolysis reaction of the unusual *ax*-$[Mn_2(CO)_9\{C(OEt)(2-C_4H_3Y)\}]$ (Y = S; O) with *n*-propylamine (*n*-Pr), *ax*-$[Mn_2(CO)_9\{C(NHn\text{-}Pr)(2-C_4H_3Y)\}]$ was obtained. Repeating the reaction with the less bulky $NH_3(g)$ resulted in the rearrangement of the carbene ligand to yield *eq*-$[Mn_2(CO)_9\{C(NH_2)(2-C_4H_3Y)\}]$ (Scheme 3.3). The same rearrangement is not

---

[25] Bezuidenhout, D.I.; Liles, D.C.; van Rooyen, P.H.; Lotz, S. *J. Organomet. Chem.* **2007**, *692*, 774.

observed for the analogous rhenium complexes; due to the increased atomic radius of a Re atom compared to the Mn atom, the Re-Re bond length is considerably longer than that of the corresponding Mn-Mn compound. The steric hindrance of the $M(CO)_5$-fragment is therefore much more pronounced in the case of manganese.
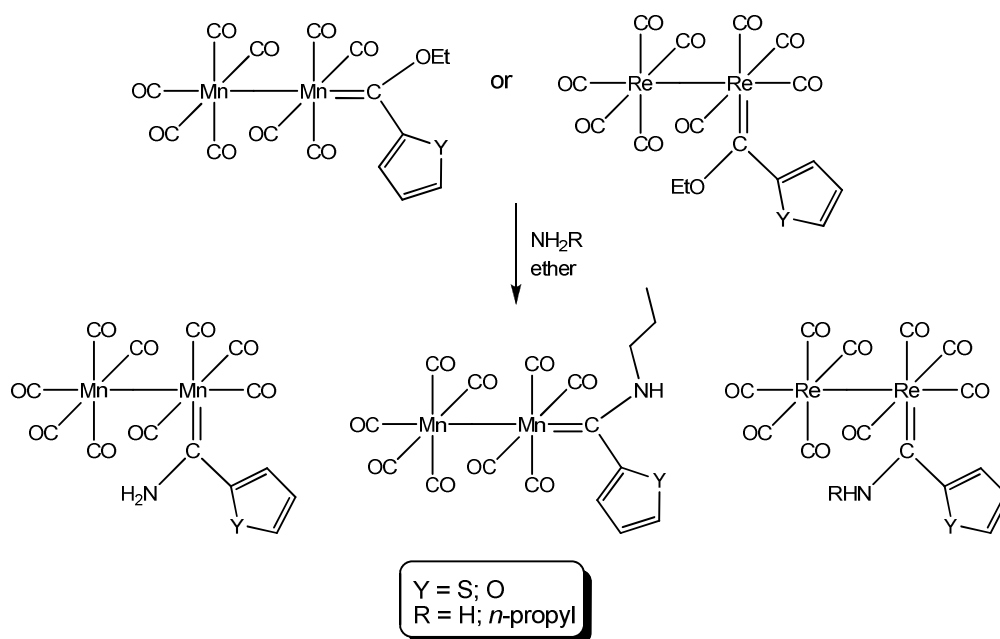
Scheme 3.3

Besides the above two examples, only one other axially substituted dimanganese nonacarbonyl monocarbene complex has been structurally characterized.[26] This complex has the unusual carbene ligand, $C(NMe_2)OAl_2(NMe_2)_5$.

In the case of rhenium, extremely bulky triphenylsilyl groups have been employed to force axial substitution as illustrated in Scheme 3.4.[27] When the study was expanded[28] to include the steric and electronic influences on bond lengths and angles at the carbene carbon, biscarbene complexes containing an axial carbene ligand on one $Re(CO)_4$-fragment, and an equatorial carbene ligand on the adjacent $Re(CO)_4$-fragment were isolated. The equatorial Re-

[26] Janik, J.Fr.; Duesler, E.N.; Paine, R.T. *J. Organomet. Chem.* **1987**, *323*, 149.
[27] Fischer, E.O.; Rustemeyer, P. *J. Organomet. Chem.* **1982**, *225*, 265.
[28] Schubert, U.; Ackermann, K.; Rustemeyer, P. *J. Organomet. Chem.* **1982**, *231*, 323.

C(carbene) bond length was found to be significantly longer (2.08(3) Å) than the axial Re-C(carbene) bond length (1.85(3) Å) when a weaker π-acceptor ligand is bonded *trans* thereto.
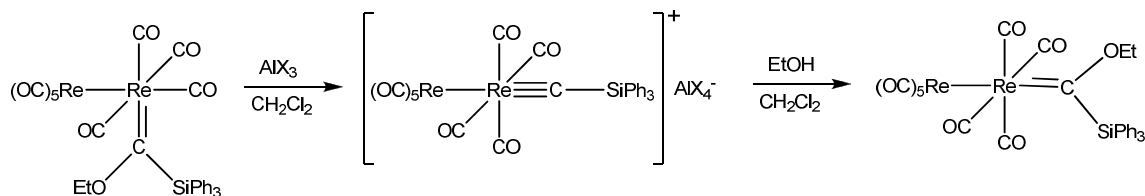
Scheme 3.4

3.1.6   Different reactivities of manganese and rhenium complexes

Previous studies in our laboratories, have shown that the reaction of lithiated $[Cr(CO)_3(\eta^5\text{-thiophene})]$ with $[Mn(CO)_5Br]$ involves attack either directly on the metal centre or on a carbonyl ligand with elimination of bromide, as shown in Scheme 3.5.[29] This yields the binuclear complexes $[Mn(CO)_5(\eta^1:\eta^5\text{-T})Cr(CO)_3]$ (T = thienyl) and $[Mn(CO)_5\{C(O)\text{-}\eta^1:\eta^5\text{-T}\}Cr(CO)_3\}]$.[30]
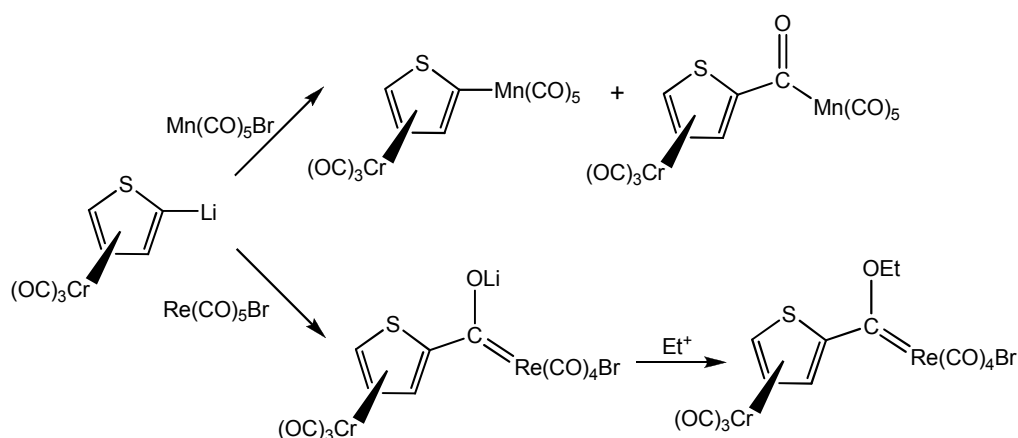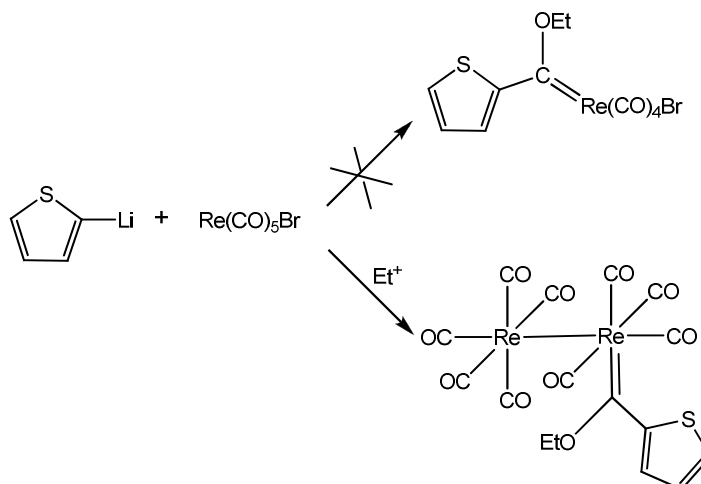

Scheme 3.5

[29] (a) Lotz, S.; Schindehutte, M.; van Rooyen, P.H. *Organometallics* **1992**, *11*, 629, (b) van Rooyen, P.H.; Schindehutte, M.; Lotz, S. *Inorg. Chim. Acta* **1993**, *208*, 207.
[30] (a) Waldbach, T.A.; van Rooyen, P.H.; Lotz, S. *Angew. Chem., Int. Ed. Engl.* **1993**, *32*, 710, (b) Waldbach, T.A.; van Eldik, R.; van Rooyen, P.H.; Lotz, S. *Organometallics* **1997**, *16*, 4056, (c) Waldbach, T.A.; van Rooyen, P.H.; Lotz, S. *Organometallics* **1993**, *12*, 4250.

In contrast (Scheme 3.5), the corresponding reaction with $[Re(CO)_5Br]$ involved attack on a carbonyl ligand without the elimination of bromide. Subsequent alkylation of the latter with Et_3OBF_4 yielded the carbene complex $[Re(CO)_4Br\{C(OEt)(\eta^1{:}\eta^5\text{-T})Cr(CO)_3\}]$.

The latter result prompted the investigation of the reaction of $[Re(CO)_5Br]$ with lithiated thiophene to assess the role, if any, of the $Cr(CO)_3$-fragment. Although not reacting smoothly, the monocarbene dirhenium nonacarbonyl complex, $[Re_2(CO)_9\{C(OEt)(2\text{-T})\}]$ was isolated and characterized after alkylation with an oxonium salt.[31] This reaction (Scheme 3.6) shows that it is possible to eliminate a bromide from $[Re(CO)_5X]$ during a Fischer carbene synthesis procedure (Li-thienyl/Et_3OBF_4) and replace it with the isolobal fragment $Re(CO)_5$ to give $[Re_2(CO)_9\{C(OEt)(2\text{-T})\}]$. In contrast, reactions of lithiated thiophene with $[Mn(CO)_5Br]$ afford a number of unstable compounds that could not be characterized unambiguously.


Scheme 3.6

The postulated mechanism of the above reaction involves the breaking of the Re-Br bond, and nucleophilic attack of the *in situ* generated $[Re(CO)_5]^-$ on the coordinatively unsaturated acyl complex, Figure 3.3, probably in a concerted

[31] Olivier, A.J. *Modification of Rhenium carbonyls with thienyl nucleophiles,* PhD. Thesis, University of Pretoria, Pretoria, **2009**.

mechanism. The mechanism parallels the findings of Norton[32] where rhenium acyl complexes only react with metal hydrides after decarbonylation (Figure 3.4). A vacant coordination site must become available on the rhenium atom bearing the acyl ligand, before the acyl complex can be attacked by [Re(CO)$_5$H].
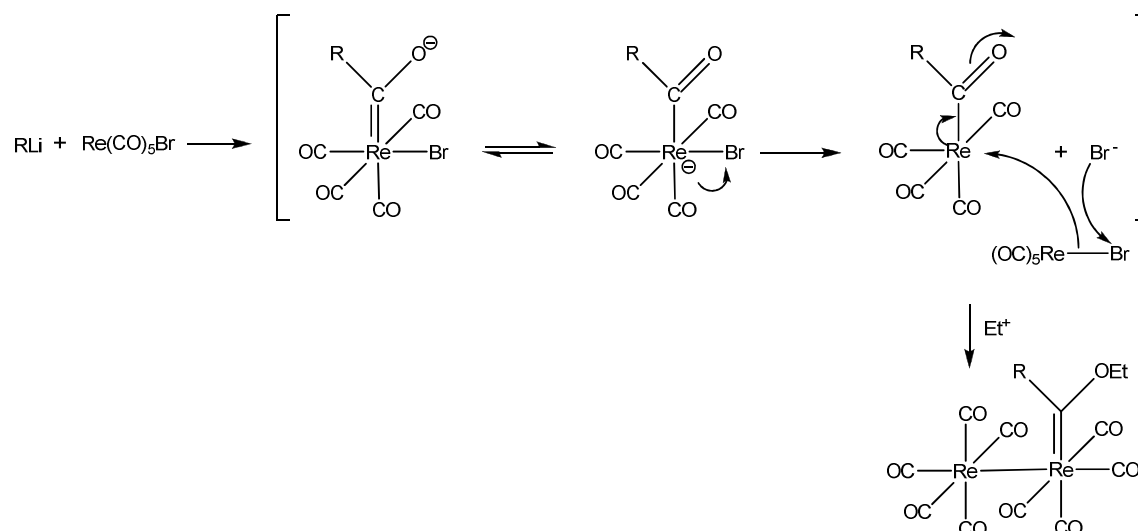
Figure 3.3   Proposed reaction mechanism for dirhenium monocarbene formation from a rhenium pentacarbonyl bromide precursor

The rhenium acyl complex undergoes nucleophilic attack at the rhenium atom by the pair of electrons in the Re-H bond, forming a species with a 3-centre, 2-electron bond. Reductive elimination yields the product aldehyde and the dinuclear rhenium complex. Neutral metal formyl complexes have also been found to transfer hydrides to metal carbonyl cations.[33]

Other kinetic studies have been conducted to investigate the reaction pathways of the Group VII metal hydrides [M(CO)$_5$H] with Group VII metal acyls [M(CO)$_5$C(O)R] (M = Mn, Re). In contrast to the proposed hydrido-acyl

---

[32] (a) Martin, B.D.; Warner, K.E.; Norton, J.R. *J. Am. Chem. Soc.* **1986**, *108*, 33, (b) Warner, K.E.; Norton, J.R. *Organometallics* **1985**, *4*, 2150, (c) Jones, W.D.; Bergman, R.G. *J. Am. Chem. Soc.* **1979**, *101*, 5447.
[33] Lin, G.-Y.; Tam, W.; Gladysz, J. *Organometallics* **1982**, *1*, 525.

intermediate found for the rhenium complexes, Halpern[34] has found that manganese reacts according to a radical mechanism.
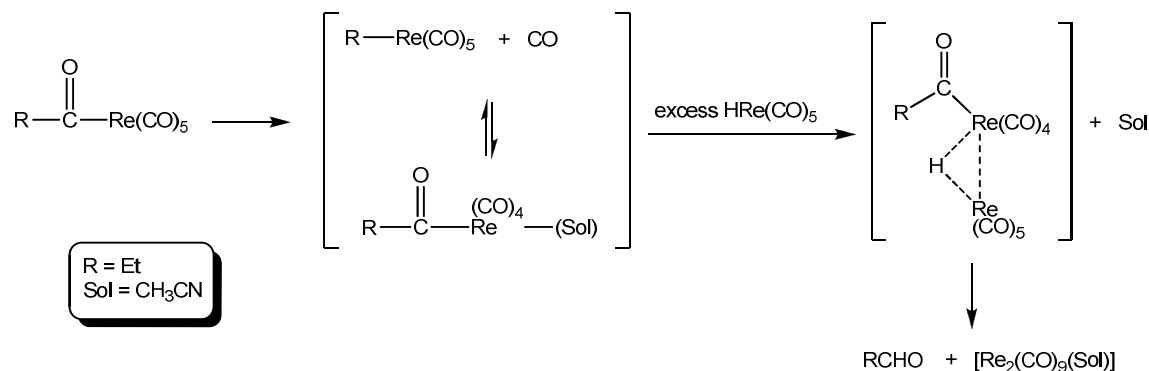
Figure 3.4   Hydrogen transfer to acyl rhenium complexes proposed by Norton[32]

## 3.1.7   Hydrido-acyl and hydroxycarbene transition metal complexes

As mentioned earlier, the site of alkylation or protonation of transition metal acylates determines the reaction pathway and composition of products and can be divided into two classes of reaction products. *O*-alkylation/protonation will leads to the formation of electrophilic carbene complexes (as seen for Group VI transition metals),[1,35] whereas metal alkylation/protonation generally favours the formation of organic products (Group VIII transition metals).[3, 4] The formation of alkyl- or hydrido-acyl transition metal complexes resulting from oxygen protonation or metal alkylation, and the subsequent elimination of these ligands affords the corresponding ketones or aldehydes.[2(c), 18(a), 36] The site of alkylation of the lithium salt of the metal acylates can be controlled or influenced by a

[34] (a) Nappa, M.J.; Santi, R.; Halpern, J. *Organometallics* **1985**, *4*, 34, (b) Sweany, R.C.; Halpern, J. *J. Am. Chem. Soc.* **1977**, *99*, 8335.
[35] (a) Fischer, E.O. *Angew. Chem.* **1974**, *86*, 651, (b) Strassner, T. *Top. Organomet. Chem.* **2004**, *13*, 4.
[36] (a) Alper, H.; Fabre, J.-L. *Organometallics* **1982**, *1*, 1037, (b) Goldberg, K.I.; Bergman, R.C. *J. Am. Chem. Soc.* **1989**, *111*, 1285, (c) Bergamo, M.; Beringhelli, T.; D'Alfonso, G.; Maggioni, D.; Mercandelli, P.; Sironi, A. *Inorg. Chim. Acta* **2003**, *350*, 475.

variety of factors such as the properties of the alkylating agent, the solvent and the electronic and steric properties of intermediates.[4(d), 36(b), 37]
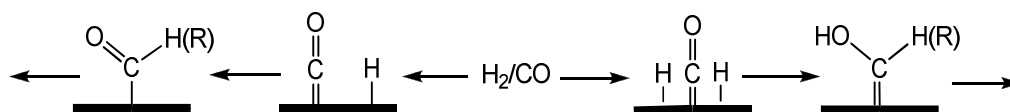
Figure 3.5   Acyl/formyl and hydroxycarbene units as potential building blocks in the Fischer-Tropsch process

Acyl/formyl and hydroxycarbene complexes (Figure 3.5) are thought to be important intermediates in CO reductions, such as found in the Fischer-Tropsch process.[38] Calculations have suggested that hydroxycarbene intermediates could also in some instances be key intermediates in hydroformylation and aldehyde decarbonylation reactions.[39]

The first transition metal hydroxycarbene complex, $[ReCp(CO)_2\{C(OH)Me\}]$ was synthesized by Fischer in 1968 by protonation of the metal acylate.[40] In view of the high reactivity of acyl alkyl or acyl hydride complexes, such species have featured as undetected intermediates in ketone and aldehyde forming reactions.[41] Examples of isolable acyl hydride complexes have been reported[42] and hydroxycarbene complexes stabilized by hydrogen bonding in the solid state have also been documented.[43] Casey *et al.* observed, during the course of

[37] Dötz, K.H.; Wenicker, U.; Müller, G.; Alt, H.G.; Seyferth, D. *Organometallics* **1986**, *5*, 2570.
[38] (a) Cornils, B.; Herrmann, W.A. Eds. *Applied Homogeneous Catalysis with Organometallic Compounds* VCH Weinheim, **1996**, (b) Muetterties, E.L.; Stein, J. *Chem. Rev.* **1979**, *79*, 479, (c) Herrmann, W.A. *Angew. Chem., Int. Ed. Engl.* **1982**, *21*, 117.
[39] Sola, M.; Ziegler, T. *Organometallics* **1996**, *15*, 2611.
[40] Fischer, E.O.; Riedel, A. *Chem. Ber.* **1968**, *101*, 156.
[41] Milstein, D. *Acc. Chem. Res.* **1984**, *17*, 221.
[42] (a) Garralda, M. A. *Dalton Trans.* **2009**, 3635, (b) Milstein, D. *Organometallics* **1982**, *1*, 1549, (c) Landvatter, E. F.; Rauchfuss, T. B. *Organometallics* **1982**, *1*, 506, (d) (e) Wang, K.; Emge, T. J.; Goldman, A. S.; Li, C.; Nolan, S. P. *Organometallics* **1995**, *14*, 4929, (f) Brockaart, G.; El Mail, R.; Garralda, M. A.; Hernández, R.; Ibarlicea, L.; Santos, J. I. *Inorg.Chim. Acta* **2002**, *338*, 249.
[43] (a) Fischer, E. O.; Kreis, G.; Kreissl, F. R. *J. Organomet. Chem.* **1973**, 56, C37, (b) Moss, J. R.; Green, M.; Stone, F. A. G. *J. Chem. Soc., Dalton Trans.* **1973**, 975, (c) Darst, K. P.; Lukehart, C. M. *J. Organomet. Chem.* **1979**, *171*, 65, (d) Chatt, J.; Leigh, G. J.; Pickett, C. J.; Stanley, D. R. *J. Organomet. Chem.* **1980**, *184*, C64, (e) Klingler, R. J.; Huffman, J. C.; Kochi, J. K. *Inorg. Chem.* **1981**, *20*, 34, (f) Casey, C. P.; Sakaba, H.; Underiner, T. L. *J. Am. Chem. Soc.*

synthesizing a rotationally restricted rhenium carbene complex having a 2-carbon link between the Cp-ligand and C(carbene) atom, an equilibrium between a hydroxycarbene complex and the isomeric metal acyl hydride complex.[44]
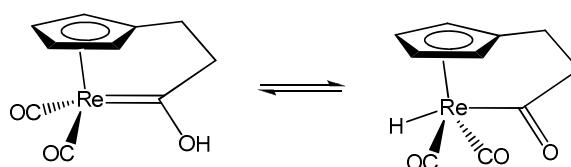
Figure 3.6   Interconversion between the Casey's[44] hydroxycarbene and acyl hydride tautomers

Although metal acyl hydrides and hydroxycarbene complexes are tautomers, no one before Casey had previously reported an observed equilibrium between the two isomers. The tautomers illustrated in Figure 3.6 are the organometallic version of the keto-enol tautomers found in organic chemistry. It was also observed that this mixture of tautomers decomposed under thermal conditions in benzene to give aldehydes.

Reactivity studies on bimetallic μ-malonyl rhenium complexes demonstrated novel carbon-carbon coupling reactions, and after cleavage and alkylation, both neutral and cationic hydroxycarbene complexes were isolated (Scheme 3.7).[45]

1991, *113*, 6673, (g) Steinborn, D.; Gerisch, M.; Bruhn, C.; Davies, J. A. *Inorg. Chem.* **1999**, *38*, 680, (h) Esterhuysen, M. W.; Raubenheimer, H. G. *Eur. J. Inorg. Chem.* **2003**, 3861.

[44] (a) Casey, C.P.; Czerwinski, C.J.; Hagashi, R.K. *J. Am. Chem. Soc.* **1995**, *117*, 4189, (b) Casey, C.P.; Czerwinski, C.J.; Fusie, K.A.; Hagashi, R.K. *J. Am. Chem. Soc.* **1997**, *119*, 3971, (c) Casey, C.P.; Czerwinski, C.J.; Powell, D.R.; Hagashi, R.K. *J. Am. Chem. Soc.* **1997**, *119*, 5750, (d) Casey, C.P.; Nagashima, H. *J. Am. Chem. Soc.* **1989**, *111,* 2352, (e) Casey, C.P.; Vosejpka, P.C.; Askham, F.R. *J. Am. Chem. Soc.* **1990**, *112*, 3713.

[45] O'Connor, J.M.; Uhrhammer, R.; Chadha, R.K.; Tsu, B.; Rheingold, A.L. *J. Organomet. Chem.* **1993**, *455*, 143.
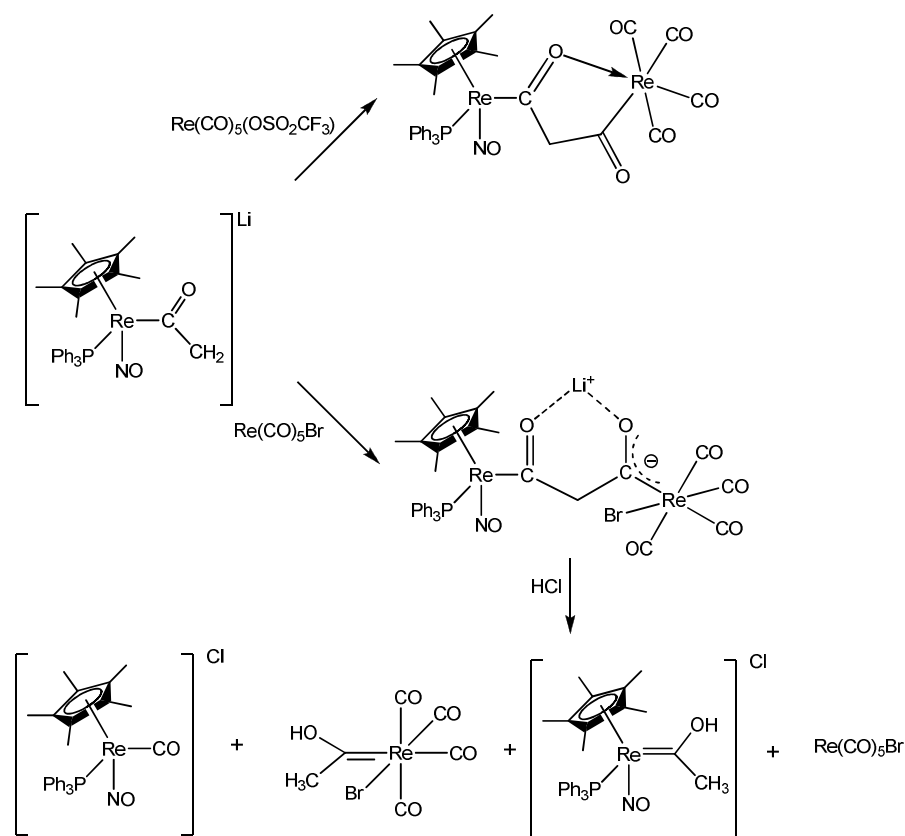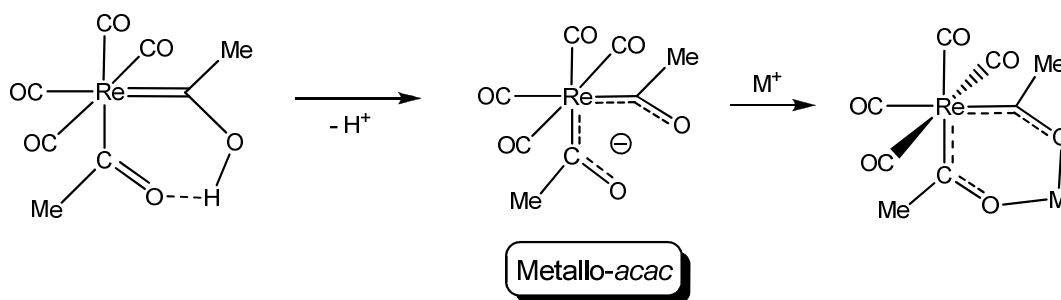
Scheme 3.7

The co-existence of a hydroxycarbene and an acyl ligand in the same monorhenium complex [Re(CO)$_4${C(O)Me}{C(OH)Me}] was reported and exploited by Lukehart and Zeile demonstrating the stabilization of a hydroxycarbene ligand through hydrogen bonding by an acyl ligand.[46] The hydroxycarbene in this complex represents the metallo-enol analogue of acetylacetone (*acac*). The deprotonated form of the metallo-organic ligand displayed coordination properties to other metal ions (Scheme 3.8).[47] Steinborn and co-workers studied similar β-diketones of platinum.[48]

---

[46] Lukehart, C. M.; Zeile, J. V. *J. Am. Chem. Soc.* **1976**, *98*, 2365.

[47] (a) Lukehart, C. M.; Torrence, G. P.; Zeile, J. V. *J. Am. Chem. Soc.* **1975**, *97* 6903, (b) Lukehart, C. M.; Torrence, G. P.; Zeile, J. V. *Inorg. Chem.* **1976**, *15,* 2393, (c) Lukehart, C. M.; Zeile, J. V. *J. Am. Chem. Soc.* **1977**, *99*, 4368.

[48] (a) Steinborn, D. *Dalton Trans.* **2005**, 2664, (b) Steinborn, D.; Schwieger, S. *Chem. Eur. J.* **2007**, *13*, 9668.
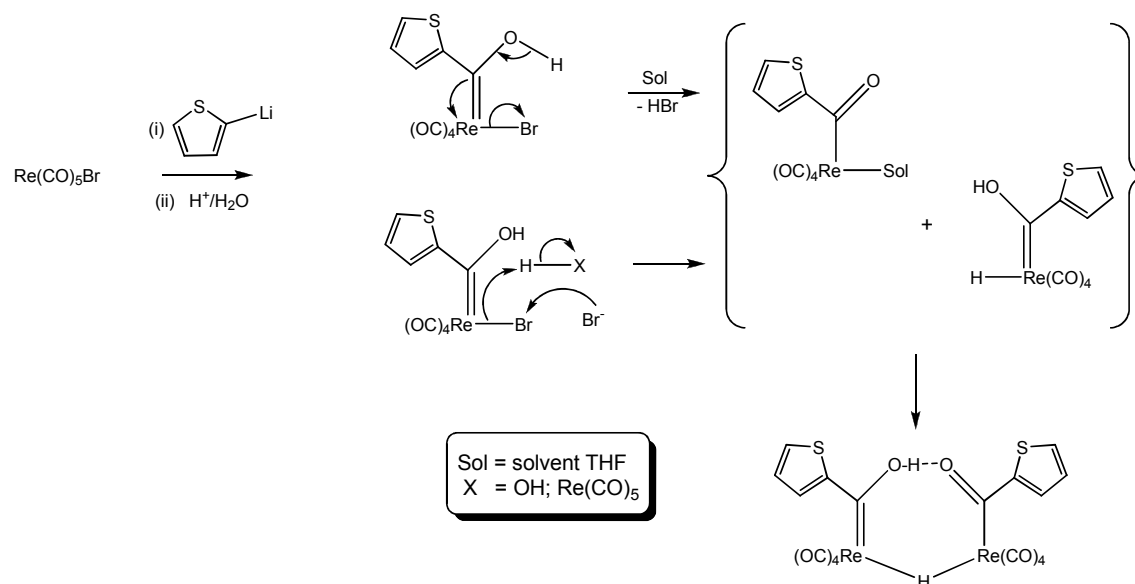
Scheme 3.8

More recently, Olivier[31] isolated and structurally characterized a hydroxycarbene-acyl complex formed from the reaction of rhenium pentacarbonyl bromide and lithiated thiophene, followed by protonation.

The complex was seen as consisting of two fragment complexes held together by a proton and a hydride, and the proposed reaction route is described in Scheme 3.9. The resemblance of this hydride acyl hydroxycarbene complex to the ruthenium Shvo catalyst[49] was emphasized: both complexes feature pendant oxygen atoms with a protonic hydrogen between them, as well as a bridging hydride.

Scheme 3.9

[49] (a) Shvo, Y.; Czarkie, D.; Rahamim, Y. *J. Am. Chem. Soc.* **1986**, *108*, 7400, (b) Casey, C.P.; Powell, D.R.; Hayashi, R.K.; Kavana, M. *J. Am. Chem. Soc.* **2001**, *123*, 1090, (c) Bullock, R.M. *Chem. Eur. J.* **2004**, *10*, 2366.

The Shvo catalyst (Figure 3.7) dissociates into a 16 electron Ru(0) and an 18 electron Ru(II) species and has found application in redox reactions, hydrogenation reactions and racemisation reaction. It contains both an hydridic hydrogen bonded to the metal, and a protonic hydrogen bonded to the ligand, and was the first ligand-metal bifunctional hydrogenation catalyst to be developed. However, only the hydride mononuclear species can be obtained if the Shvo catalyst is reacted with H_2 or formic acid.[50] Therefore inefficient use of the ruthenium metal is made, because much of it is present as the diruthenium species which is not active in reduction.[51]
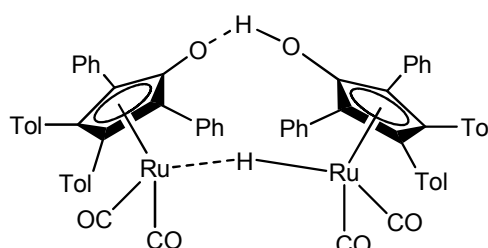

Figure 3.7   The Shvo catalyst

3.2   **Results and discussion**

3.2.1   **Focus of this study**

The range of Group VI cluster carbene complexes synthesized in Chapter 2 was extended by making use of mononuclear manganese (in the form of cyclopentadienyl dicarbonyl manganese) as the central metal, and the carbene substituents employed were ferrocene (bonded directly to the carbene carbon atom) as well as ethyl or titanocene chloride (bonded to the carbene oxygen atom). As before, both the mono- and the corresponding biscarbene complexes were synthesized, and are illustrated in Figure 3.8.

---

[50] Casey, C.P.; Singer, S.W.; Powell, D.R. *Can. J. Chem.* **2001**, *79*, 1002.
[51] Casey, C.P.; Beetner, S.E.; Johnson, J.B. *J. Am. Chem. Soc.* **2008**, *130*, 2285.
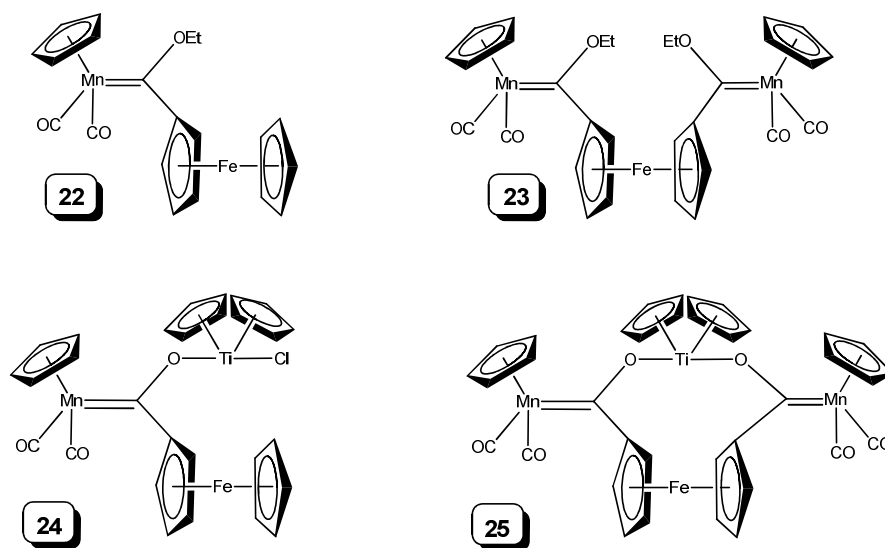
Figure 3.8   Manganese carbene complexes synthesized

Next, the possibility of increasing the number of metal fragments in the cluster complexes was investigated by employing the dinuclear Group VII binary metal carbonyl, $Re_2(CO)_{10}$ as precursor central metal. A variety of products consisting of both mono- and dirhenium complexes indicated a mixture of the dirhenium acylate precursor and other species resulting from Re-Re bond cleavage during this stage of the reaction. Depending on the site of alkylation/metalation/protonation, a range of di- and monorhenium Fischer carbene complexes and other products could be isolated. The acyl and hydrido intermediates formed, as well as hydroxycarbene complexes are precursors to aldehyde formation. Figure 3.9 lists all the rhenium metal-containing product complexes isolated from the rhenium synthesis reactions in this chapter.
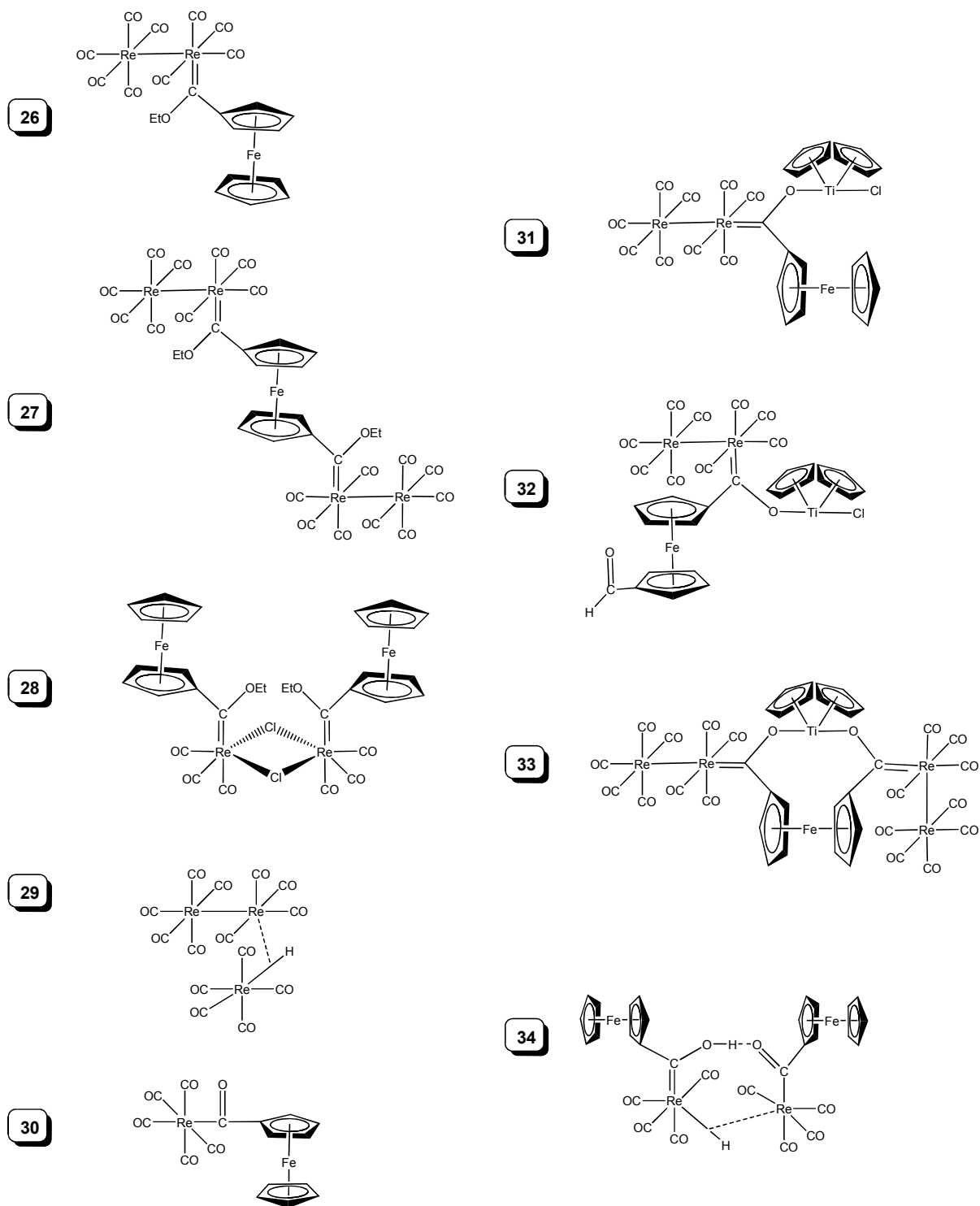
Figure 3.9   Complexes obtained from rhenium reactions

3.3 Synthesis

3.3.1 Synthesis of cyclopentadienyl manganese carbene complexes

For Group VII transition metals, carbene complexes with cyclopentadienyl as an auxiliary ligand, are readily accessible.[52] The corresponding biscarbene complexes can also be obtained by intermolecular oxidative coupling in the presence of anhydrous $FeCl_3$,[52(a)] as shown in Scheme 3.10.
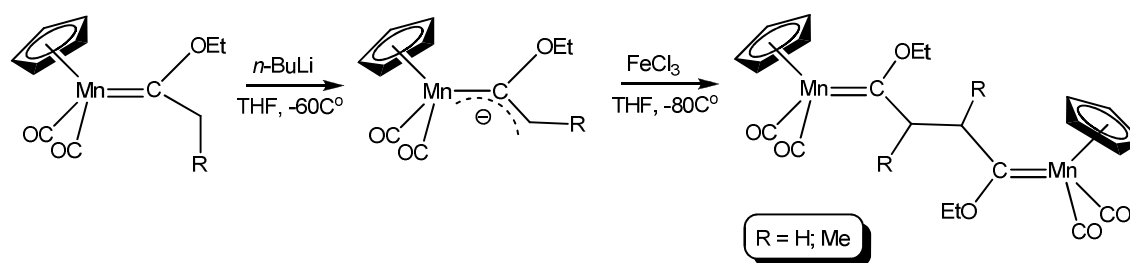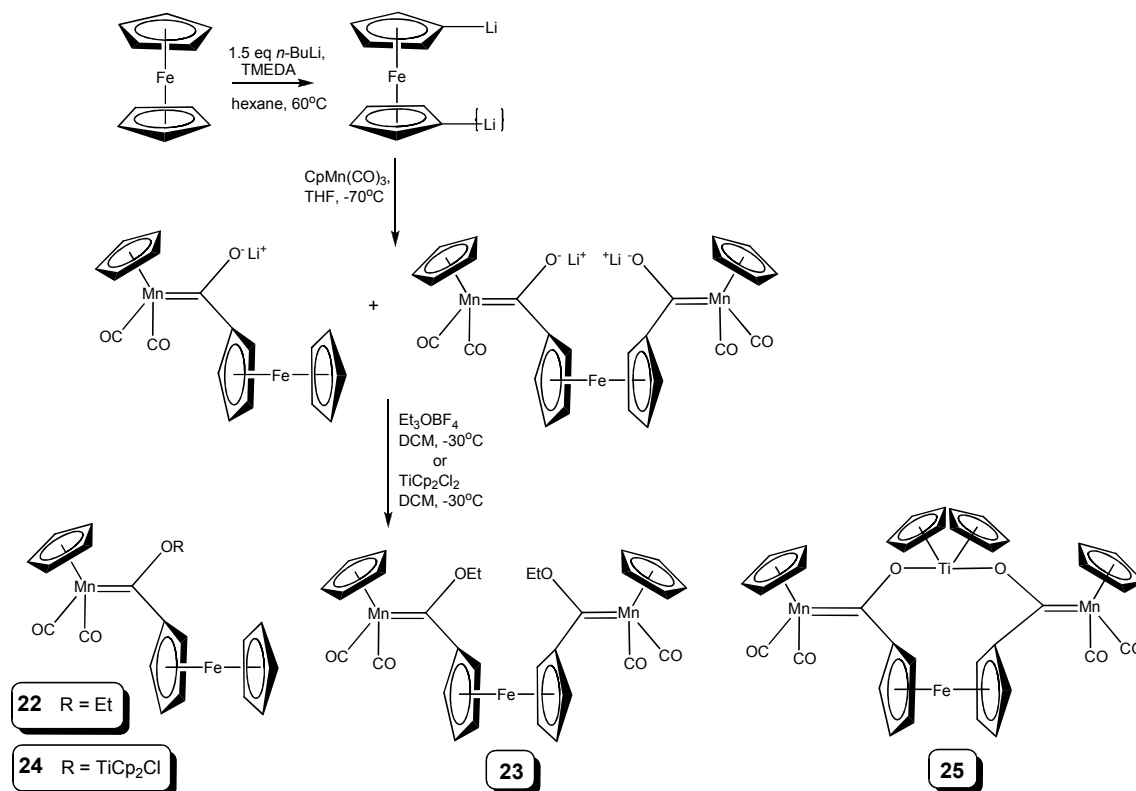

Scheme 3.10

As with the Group VI transition metals Cr and W, the monocarbene complex of methylcyclopentadienyl manganese with ferrocenyl and ethoxy substituents on the carbene ligand has been synthesized before.[22] The analogous complex [MnCp(CO)$_2${C(OEt)Fc}] (**22**) was synthesized in this study for the purpose of comparison. The general procedure followed involved reaction of *n*-BuLi with ferrocene to yield both the mono- and dilithiated precursors, followed by the addition of [MnCp(CO)$_3$] in THF at low temperatures. Alkylation with Et$_3$OBF$_4$ in dichloromethane yielded complex **22** and the novel biscarbene complex **23** [μ-Fe{C$_5$H$_4$C(OEt)MnCp(CO)$_2$}$_2$]. Alternatively, metalation with titanocene dichloride yielded, the monocarbene complex **24** [MnCp(CO)$_2${C(OTiCp$_2$Cl)Fc}] and the bridging bisoxy titanocene and bridging ferrocen-1,1'-diyl complex **25** [{μ-

[52] (a) Rabier, A.; Lugan, N.; Mathieu, R. *J. Organomet. Chem.* **2001**, *617 - 618*, 681, (b) Casey, C.P.; Kraft, S. ; Powell, D.R. ; Kavana, M. *J. Organomet. Chem.* **2001**, *617 – 618*, 723.

TiCp$_2$O$_2$-O,O'}{μ-Fe(C$_5$H$_4$)$_2$-C,C'}[CMnCp(CO)$_2$}$_2$]. The Fischer procedure for the preparation of the above complexes is summarized in Scheme 3.11.

Scheme 3.11

3.3.2 Synthesis of dirhenium ethoxycarbene complexes

Lithioferrocene can be prepared either by direct abstraction of a proton from ferrocene by butyllithium[53] or by an exchange reaction between chloromercuriferrocene and butyllithium.[54] The former route leads to a mixture of mono- and dilithiated ferrocene, usually with a low yield of FcLi. The latter route is complicated by the possibility of the formation of both alkylated and mercury-

---

[53] (a) Benkeser, R.A.; Goggin, D.; Schroll, G.A. *J. Am. Chem. Soc.* **1954**, *76*, 4025, (b) Mayo, D.W.; Shaw, R.D.; Rausch, M. *Chem. Ind.* London, **1957**, 1388.

[54] (a) Helling, J.F.; Seyferth, D. *Chem. Ind.* London, **1961**, 1568, (b) Seyferth, D.; Hoffman, H.P.; Burton, R.; Helling, J.F. *Inorg. Chem.* **1962**, *1*, 227, (c) Hedberg, F.L.; Rosenberg, H. *Tetrahedron Lett.* **1969**, *46*, 4011.

containing derivatives of ferrocene as undesired side products. After the former method was employed in our laboratory with no appreciable yield of FcLi, it was decided to use halogen-metal exchange of iodoferrocene and n-BuLi to afford the monolithiated product in high yield. Fish and Rosenblum's method[55] was followed to prepare FcI, and the exchange reaction of a stoichiometric amount of n-butyllithium in ether at -70°C resulted in a high yield of FcLi with no concurrent dilithiation. Subsequent metalation with $Re_2(CO)_{10}$ in THF at -50°C, followed by alkylation with Et_3OBF_4 in dichloromethane yielded the dark red complex $[Re_2(CO)_9\{C(OEt)Fc\}]$ (**26**). Unreacted $Re_2(CO)_{10}$ and ferrocene were separated from the reaction mixture by column chromatography. Only one dark red band was isolated besides the unreacted starting materials. However, NMR spectroscopy revealed duplication of all the ^1H and ^{13}C chemical shifts. The IR spectrum also displayed more carbonyl stretching vibration bands than expected, many of the bands overlapping. From this information, we concluded that a mixture of the equatorial and the axial isomers were present in solution, as the steric bulk of the ferrocenyl substituent could force the electronically unfavoured axial substitution. Unfortunately, the two different isomers could not be separated and purified, possibly due to the fact that the isomers are in equilibrium in solution.
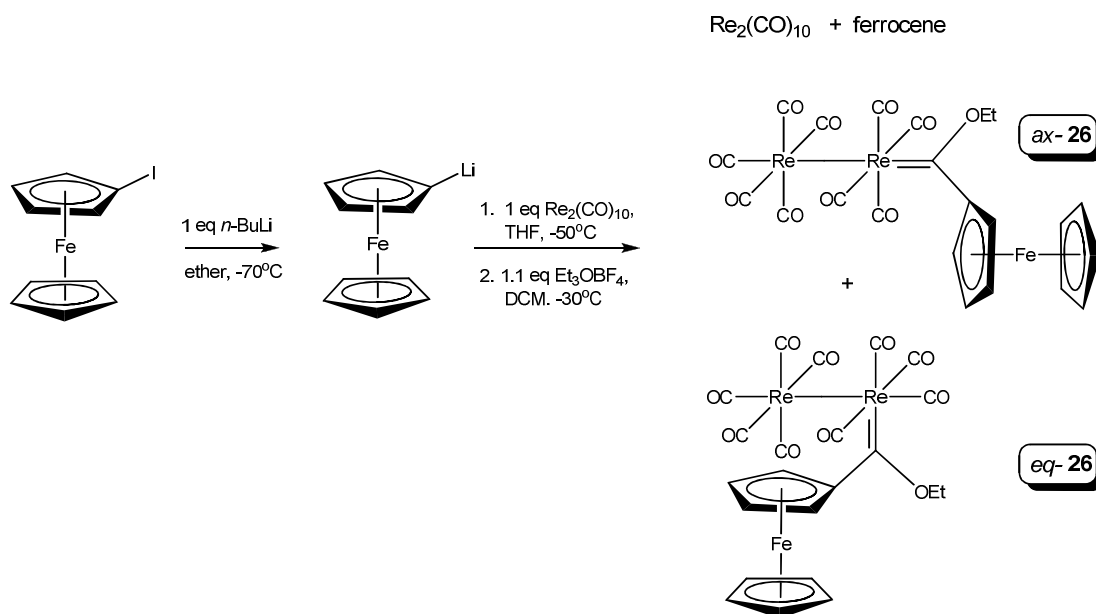
Figure 3.10   Synthesis of *ax*- and *eq*-$[Re_2(CO)_9\{C(OEt)Fc\}]$

---

[55] Fish, R.W.; Rosenblum, M. *J. Org. Chem.* **1965**, *30,* 1253.

For the preparation of **27**, the corresponding biscarbene complex to **26**, ferrocene was readily dilithiated with *n*-BuLi and TMEDA in hexane at 45°C. The dilithiated species precipitate out of the solution as an orange solid and the yield relative to the monolithiated species could be increased (> 80%) by removal of the solution *via* canula. After solvent evaporation and cooling to -50°C, 2 mole eq of dirhenium decacarbonyl was added in THF, and alkylation with 2 mole eq of alkylating agent yielded, besides unreacted rhenium carbonyl, three fractions identified by thin layer chromatography. The two products eventually obtained by column chromatography are illustrated in Scheme 3.12.
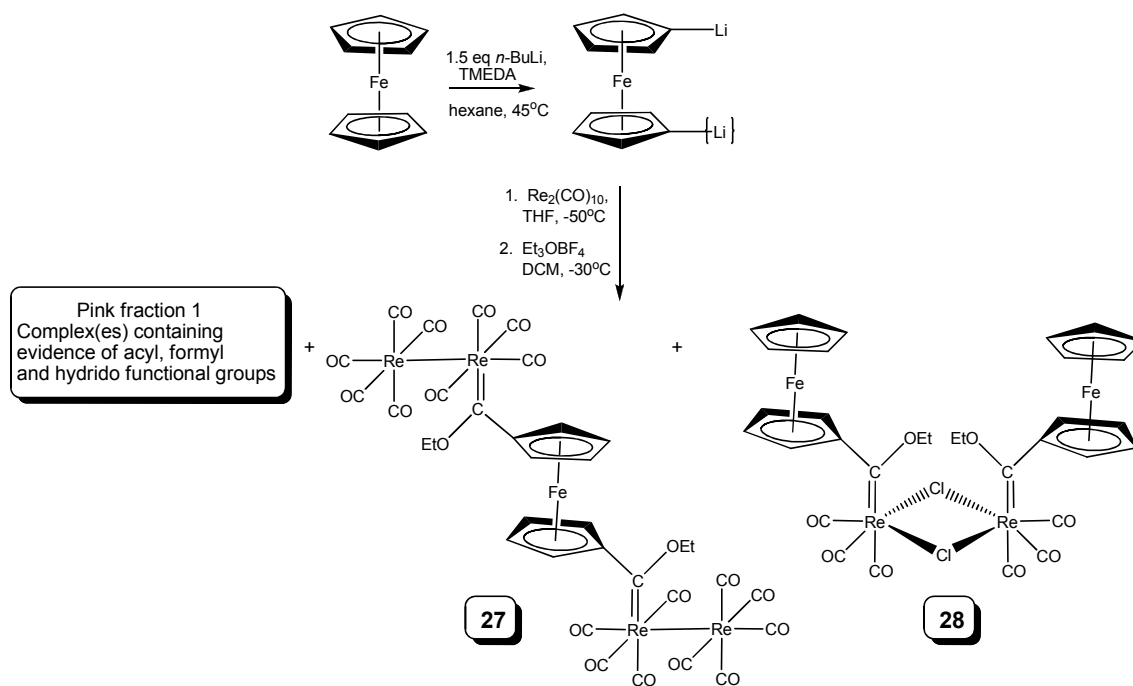
Scheme 3.12

The first pink fraction to be eluted from column chromatography on silica gel could not be successfully characterized before decomposition. The IR spectrum of the compound therein showed four υ(CO) bands at 2102 (m), 2038 (s), 1994 (vs) and 1939 (s) cm^{-1}, but over time, new bands appeared (overlapping with the previous bands) at 2087 and 1968 cm^{-1}. From the ^{13}C NMR spectrum, a carbene signal of strong intensity could be assigned at 308.1 ppm. However, more than

the expected number of ferrocenyl resonances (in the range of 72 -78 ppm), ethoxy resonances and carbonyl resonances (186 – 199 ppm) were observed. In addition, two acyl-like chemical shifts at δ = 286.5 and 274.9 were seen, but the corresponding C-O stretches (that would appear in the range of 1500-1700 cm^{-1} of the infrared spectrum) were not observed. Furthermore, the proton NMR spectrum displayed a very downfield shift at 9.20 ppm, usually associated with an aldehyde functional group, as well as a very highfield chemical shift at -13.70 ppm. For most monorhenium complexes the hydride signal is seen in the range -4 to -10 ppm[44(a), 56] and for the dirhenium complexes or rhenium clusters with a bridging hydride, the signal commonly seen is in the range of -14 to -20 ppm.[57] Although thin layer chromatography revealed the presence of only one compound, the possibility of more than one complex present could not be ruled out. Decomposition of the formed products with loss of the metal carbonyl moiety to yield compounds such as FcCHO is, however, the most probable event.

The contents of the next band was collected as a bright red compound, which was identified by single crystal X-ray crystallography as being *fac*-[(μ-Cl)$_2$-(Re(CO)$_3${C(OEt)Fc})$_2$] (**28**). Finally, the expected product, dark brown complex *eq,eq*-[μ-Fe{C$_5$H$_4$C(OEt)Re$_2$(CO)$_9$}$_2$] (**27**), was eluted as the third fraction in a yield of 38%. Unlike the monocarbene analogue, no evidence of an axial isomer was observed.

Complex **28** displays some similarities to the acyl-hydrido hydroxycarbene dirhenium complex:[31] in both cases, cleavage of the Re-Re bond of the precursor Re$_2$(CO)$_{10}$ has occurred. The complex can be seen as made up of two coordinatively unsaturated [Re(CO)$_3${C(OEt)Fc}Cl]-fragments. If employing the same approach as demonstrated in Scheme 3.9, a possible reaction route can be proposed as in Scheme 3.13.

---

[56] Krumper, J.R.; Martin, R.L.; Hay, P.J.; Yung, C.M.; Veltheer, J.; Bergman, R.G. *J. Am. Chem. Soc.* **2004**, *126*, 14804.
[57] (a) Adams, R.D.; Captain, B.; Hollandsworth, C.B.; Johansson, M.; Smith, Jr., J.L. *Organometallics* **2006**, *25*, 3848, (b) Adams, R.D.; Kwon, O.-S.; Perrin, J.L. *J. Organomet. Chem.* **2000**, *596*, 102.
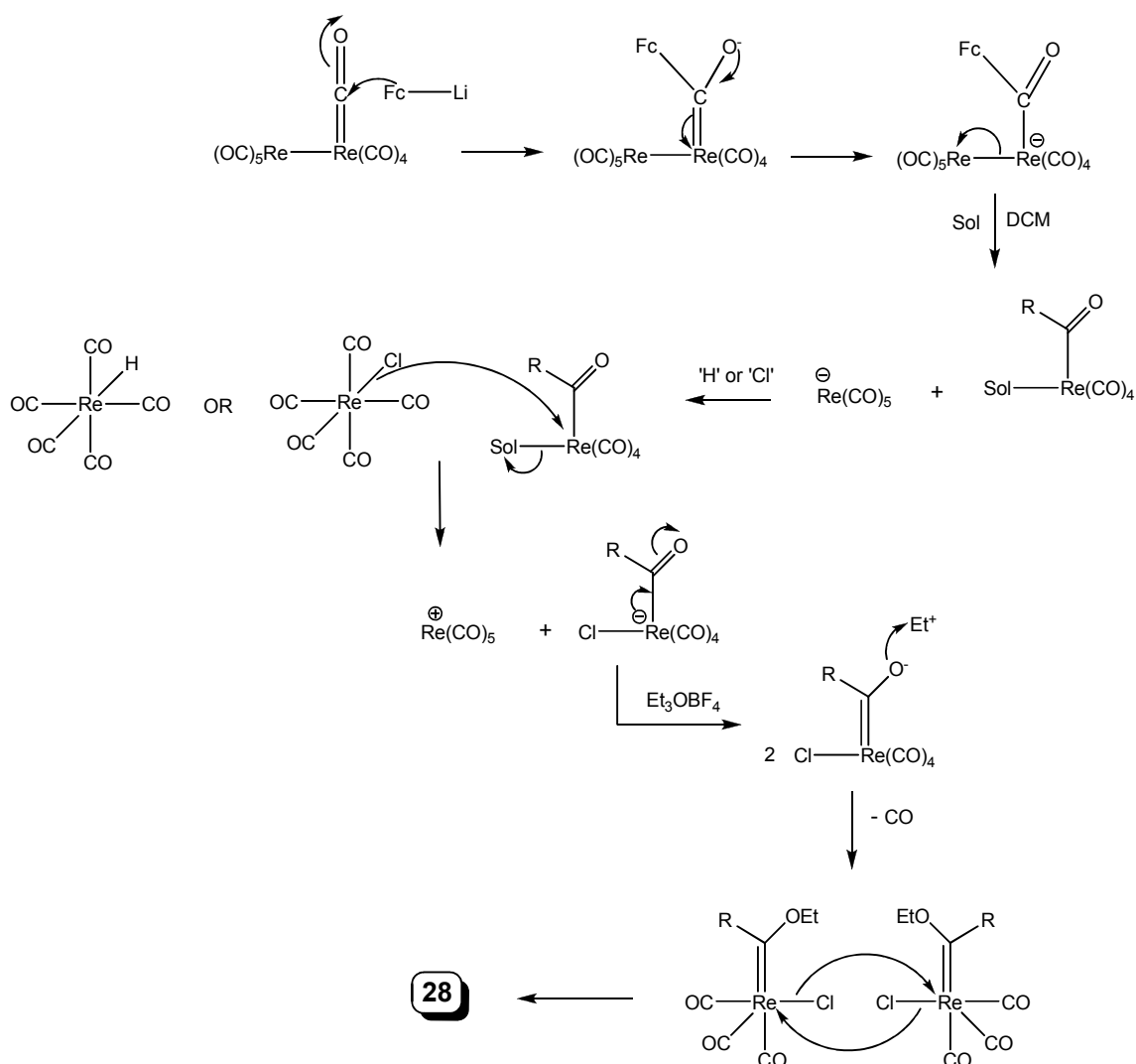
Scheme 3.13

1,1'-dilithioferrocene attacks on a carbonyl ligand of $[Re_2(CO)_{10}]$ and imparts a negative charge to the complex, stabilized by resonance as the metal acylate. The formation of this anionic intermediate facilitates the loss of the $Re(CO)_5$-fragment and the Re-Re bond breaks heterolytically, and a solvent (THF) molecule coordinates to the vacant site.[32] The other fragment, the $[Re(CO)_5]^-$ anion, abstracts a chlorine atom from solvent dichloromethane, as this is the only chlorine source available. Evidence of chlorine abstraction from dichloromethane in a radical mechanism by a tetrahedrane cluster $[RCCo_2Mo(\eta^5\text{-indenyl})(CO)_8]$ (R = H; Ph), after breaking of the Mo-Co and Co-

Co bond, has recently been published by Watson *et al.*[58] Reaction of a ruthenium carbonyl complex $[Ru_2(CO)_2(\mu\text{-}CO)H(\mu\text{-}CCPh)(\mu\text{-}dppm)_2]$ with chlorinated solvent CH_2Cl_2 also resulted in ligand substitution by a solvent chlorine atom to give $[Ru_2(CO)_2(\mu\text{-}CO)Cl(\mu\text{-}CCPh)(\mu\text{-}dppm)_2]$.[59]

From literature, Mn-X bond dissociation energies can be ordered as follows:[60] $(CO)_5Mn\text{-}X$ [$\Delta(Mn\text{-}X)$, kJ.mol^{-1}] X = Br (280) > H (250) > Ph (sp^2-C) (205) > CH$_3$ (sp^3-C) (185) > C(O)CH$_3$ (165) > Mn(CO)$_5$ (160). Re-X bonds are approximately 20% stronger and according to the above approximate values, a Re-Cl bond would be much stronger than a Re-Re bond. The chloro ligand is therefore transferred to the [(Sol)-Re(CO)$_4$\{C(O)Fc\}] complex, and after alkylation and decarbonylation, two of the resultant coordinatively unsaturated *fac*-[Re(CO)$_3$\{C(OEt)Fc\}Cl]-fragments form chloro-bridges to yield complex **28**.

It is possible, too, that the rhenium pentacarbonyl anion can abstract a hydrogen atom by the same mechanism, yielding the rhenium pentacarbonyl hydride complex, another byproduct identified along with the rhenium pentacarbonyl chloride complex.

### 3.3.3 Synthesis of dirhenium carbene cluster complexes

The same procedure as described in Section 3.3.2 above was employed to synthesize the titanoxycarbene complexes, the only difference being metalation of the acyl metalate with titanocene dichloride in dichloromethane, instead of alkylation with an oxonium salt.

Before alkylation/metalation, the lithiated salt can be represented as either a rhenium acylate (**A**) that can be converted to the rhenium carbonyl anion (**B**) and an acyl rhenium complex (**C**), respectively (Figure 3.11).

[58] Watson, W.H.; Poola, B.; Richmond, M.G. *J. Organomet. Chem.* **2006**, *691*, 5567.
[59] Kuncheria, J.; Mirza, H.A.; Vittal, J.J.; Puddepatt, R.J. *J. Organomet. Chem.* **2000**, *593 – 594*, 77.
[60] (a) Connor, J.A. *Top. Curr. Chem.* **1977**, *71*, 71, (b) Collman, J.P.; Hegedus, L.S.; Norton, J.R.; Finke, R.G. *Principles and Application of Organotransition Metal Chemistry,* Oxford University Press, Mill Valley, CA, **1987**.
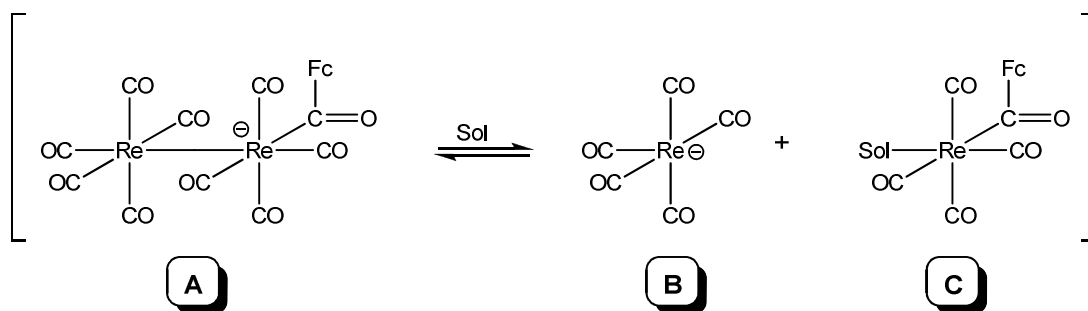
Figure 3.11   Re-acylate (**A**), Re(CO)$_5^-$ (**B**) and Re-acyl (**C**) intermediates

Thin layer chromatography, after complexation with TiCp$_2$Cl, revealed the presence of nine different compounds, and these were separated and purified on an alumina column, and will be discussed in the order of elution from the column. The formation of the minor byproducts isolated from the reaction mixture can mostly be ascribed to the transfer of a proton by two possible mechanisms, either ionic or radical. Firstly, transfer of a proton from dichloromethane or other proton source *via* a radical mechanism, or the protonation of the rhenium pentacarbonyl anion, [Re(CO)$_5$]$^-$ (**B**) to give [Re(CO)$_5$H]. Hydrolysis of the rhenium complexes occurs both in reaction mixture solvent THF or dichloromethane, as well as on the silica gel columns during chromatography if trace amounts of water are present. The *in situ* formation of [Re(CO)$_5$H] was noted in NMR studies and the secondary product, the trirhenium hydride [Re$_3$(CO)$_{14}$H] (**29**) was isolated. More important was the subsequent hydrogen transfer reaction of [Re(CO)$_5$H] with the corresponding neutral ferrocene-acyl complex of rhenium. The products also contained some ferrocenyl aldehydes or acyl complexes.

Re$_2$(CO)$_{10}$ + Li—Fc
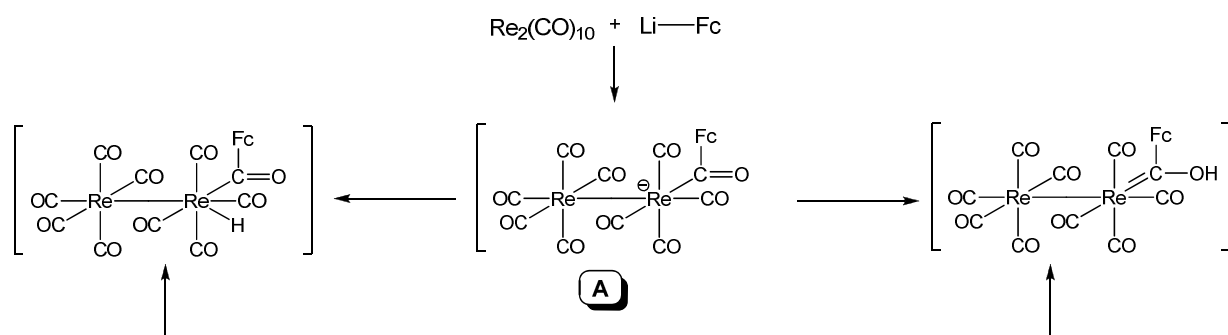
Scheme 3.14

The first band eluted contained the colourless starting material Re$_2$(CO)$_{10}$. After this followed the second fraction, pink in colour. IR spectroscopy clearly displayed carbonyl stretches in the expected range, and the presence of the unique hydroxycarbene-acyl complex [(μ-H)$_2$-(Re(CO)$_4${C(O)Fc})$_2$] (**34**), identified as the molecular ion peak in a mass spectrum, indicated a similar mechanism as was discussed by Olivier.[31] The postulated reaction pathway for the formation of **34** is shown in Figure 3.11 and Schemes 3.14 and 3.15.

The formation of **34** is interesting and can be seen as originating from **B** and **C** (Scheme 3.15) by a hydrogen transfer process from [Re(CO)$_5$H] to the acyl fragment after metal alkylation. This is then comparable to a similar process studied kinetically by Norton.[32] An intramolecular transfer of the hydrogen atom from the rhenium to the oxygen will result in the formation of an acyl-hydride that is in equilibrium with the hydroxycarbene ligand. Cleavage of the Re(CO)$_5$-fragments form the building blocks of **34**.

106
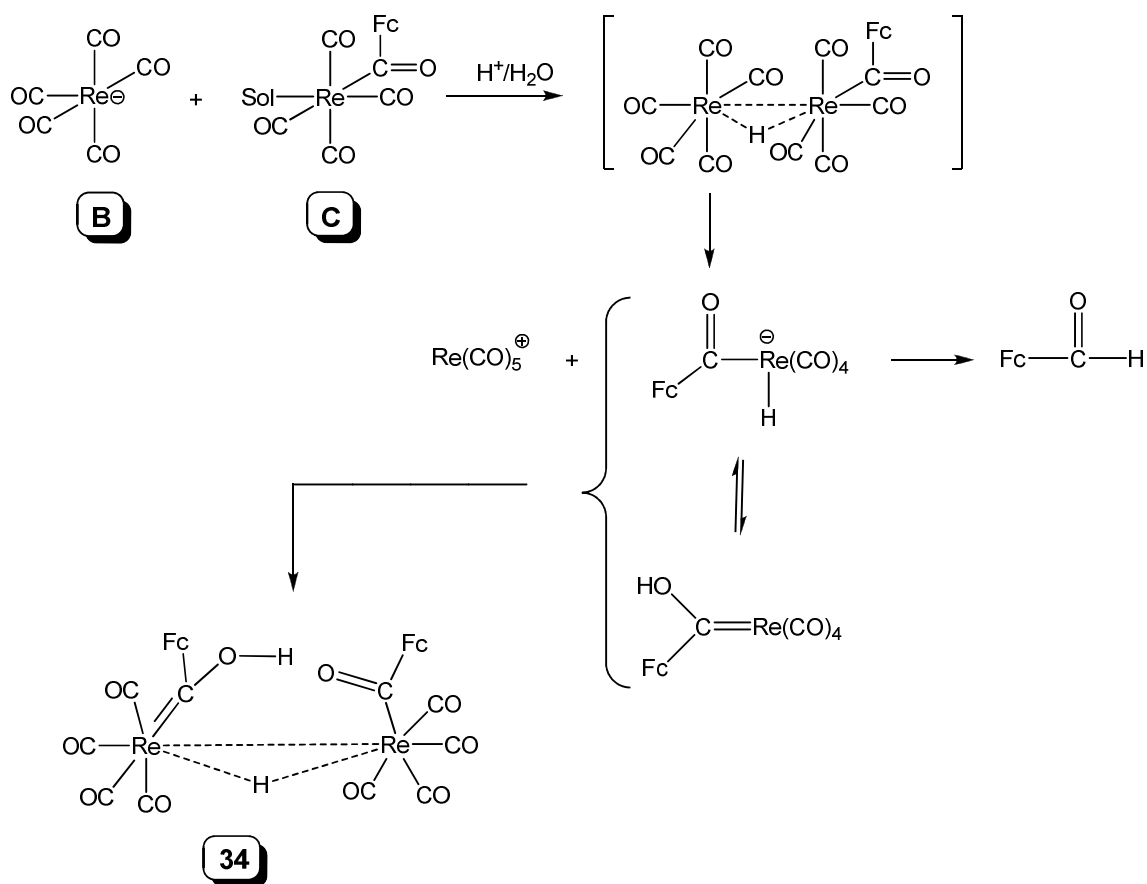
Scheme 3.15

This H-transfer is, however, only one mechanistic possibility for the formation of **34**. Protonation of the initial rhenium acylate, for example after alkylation with Et$_3$OBF$_4$ or metalation with TiCp$_2$Cl$_2$, subsequent hydrolysis reaction during column chromatography can also result in the obtained product. As mentioned before, the equilibrium between the hydroxycarbene and hydrido-acyl intermediates for rhenium cyclopentadienyl complexes has been previously studied and reported by Casey.[44] Unlike in the Casey studies, no monorhenium hydroxycarbene or hydrido-acyl complexes could be isolated and it was assumed that the equilibrium whereby the hydroxycarbene was converted into the acyl-hydride intermediate was favoured.

Complex **34** decomposed in the course of a few days, and subsequent NMR spectroscopy and X-ray diffraction identified one of the decomposition products as biferrocene.[61] The formation of this dimeric byproduct can be rationalized by the ionic nature of the titanoxy substituent, which would favour the rhenium acylate form of the intermediate (Figure 3.11) because of enhanced backbonding from the anionic oxygen to the electrophilic carbene carbon. The ionic nature of titanoxycarbene complexes is supported by structural studies (Chapter 2) and in this study, by the ease of acyl decomplexation. Thus the titanoxycarbene complex acts as an acyl synthon similarly to the situation observed by Barluenga and co-workers for $[Mo(CO)_5\{C(OBX_2)R],$[62] illustrated in Figure 3.12.
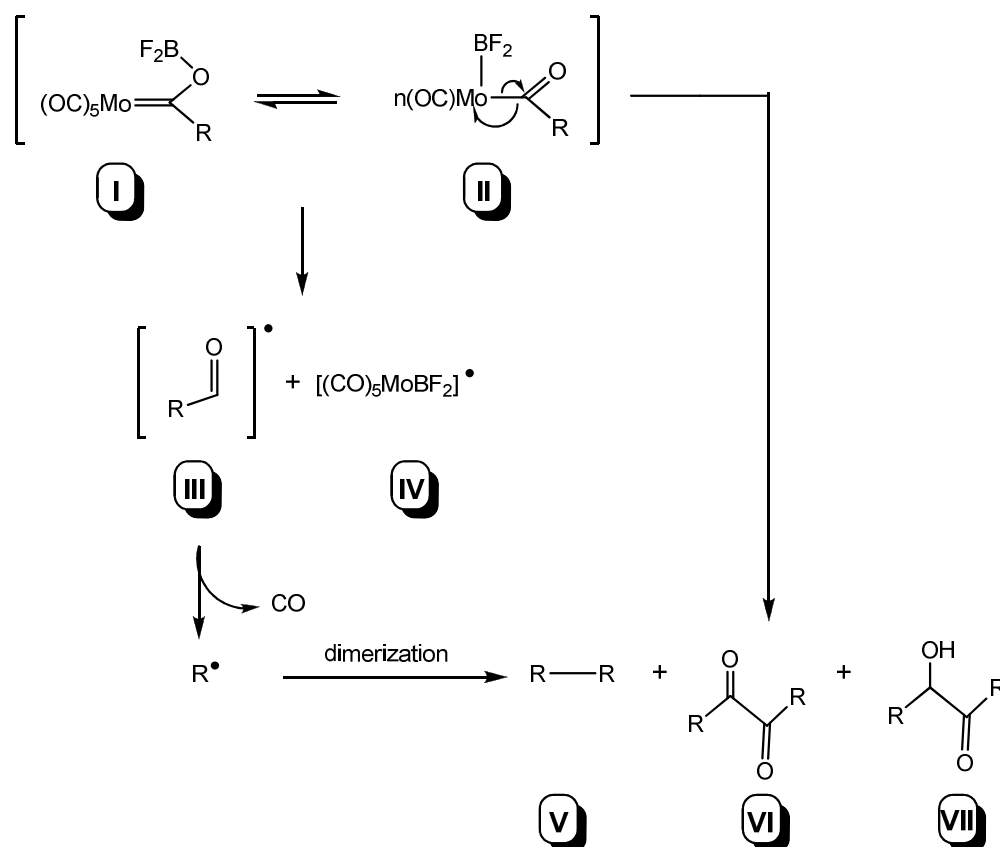

Figure 3.12   Mechanism for the formation of dimerization product **V**

[61] (a) Rausch, M.D.; Vogel, M.; Rosenberg, H. *J. Org. Chem.* **1957**, *22*, 900, (b) Rausch, M.D. *J. Am. Chem. Soc.* **1960**, *82*, 2080.
[62] Barluenga, J.; Rodríguez, F.; Fañanás, F.J. *Chem. Eur. J.* **2000**, *6*, 1930.

Homolytic scission of the carbon-metal bond of **II** leads to the acyl radical **III** and the radical species **IV**. Formation of the dimer **V** can be understood as the result of the decarbonylation[63] of **III** and dimerization of the radical species thus obtained.

The third fraction (orange) was spectroscopically characterized as containing formylferrocene (FcCHO), both by its NMR spectra as well as the characteristic C=O vibration in the IR spectrum at 1681 cm^{-1}.[64] Once again, the two possible routes towards formation of FcCHO involves either hydrogen transfer (as illustrated in Scheme 3.13) to the rhenium acylate intermediate (**C**) in Figure 3.11, which can be inferred to yield the product aldehyde after reductive elimination of this ligand. The other possibility involves hydrolysis of the carbene ligand, after which the hydroxycarbene intermediate is converted to the acyl hydride intermediate, as shown in Scheme 3.16. Acyl-hydride elimination is initiated by the reaction of trace amounts of water during chromatography.
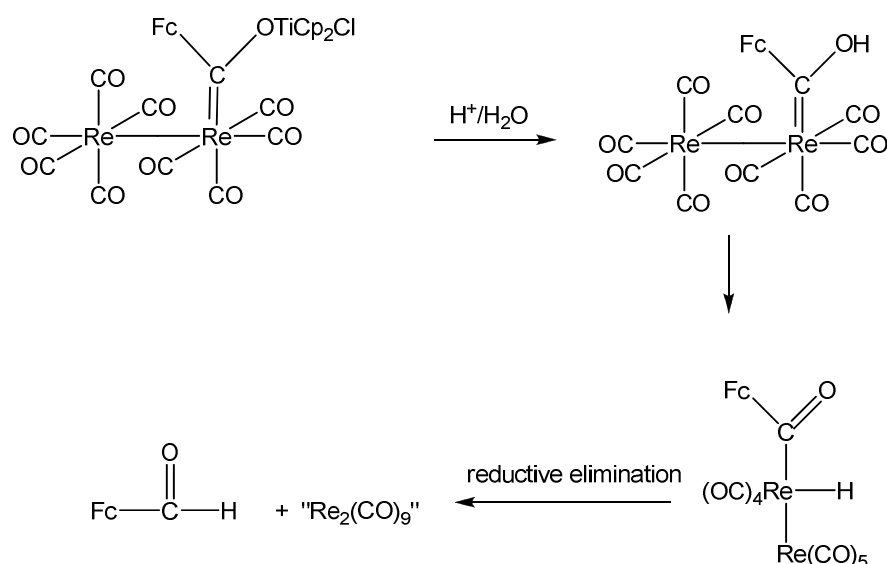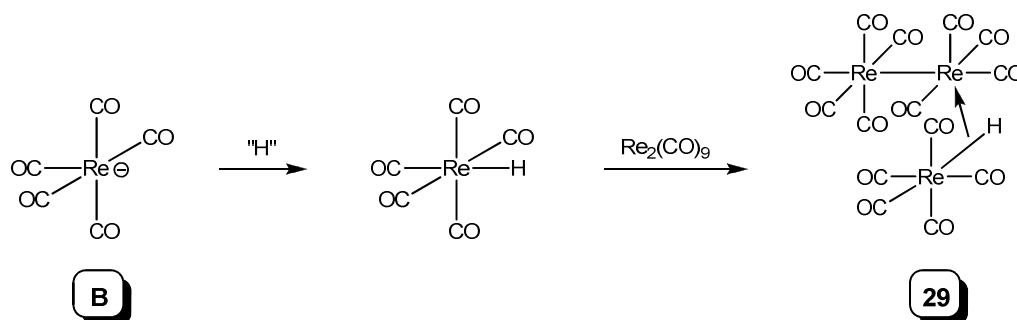

Scheme 3.16

[63] (a) Ryu, I.; Sonoda, N. *Angew. Chem., Int. Ed. Engl.* **1996**, *35*, 1050, (b) Chatgilialoglu, C.; Crich, D.; Komatsu, M. ; Ryu, I. *Chem. Rev.* **1999**, *99*, 1991.
[64] (a) Rosenblum, M. *Chem. Ind.* **1957**, *3*, 72, (b) Kamezawa, N. *Journal of Magnetic Resonance* **1973**, *11*, 88.

The fourth band eluted was light yellow in colour. Initially, no ^{1}H NMR signals could be detected for this compound. However, the IR spectrum revealed the existence of many carbonyl stretches. Final confirmation of the structure of this compound (**29**) was obtained by X-ray crystallography, and the complex was identified as the Fellman-Kaesz complex [$Re_3(CO)_{14}H$].[65] Re-investigation of the proton NMR spectrum then yielded the expected extreme upfield hydride shift (Table 3.4) at δ: -15.41.

The complex **29** has also been obtained previously in approximately 50% yield from the photochemical reaction of dirhenium decacarbonyl and triphenylsilane[66] or thiophene.[67] The complex can be viewed as a $Re(CO)_5$- and a $Re_2(CO)_9$-fragment bridged by a hydrido ligand. Byers and Brown have suggested a radical mechanism for the formation of this complex, either from $Re_2(CO)_9H$- and $Re(CO)_5$-radicals, or from $Re_2(CO)_9$ and $Re(CO)_5H$. This would support the finding of dimerization to yield biferrocene as discussed before. The transfer of a proton from dichloromethane (solvent) to the reactive rhenium carbonyl anion was indicated by a control NMR spectrum of the reaction mixture immediately before alkylation, and the proposed reaction pathway for the formation of **29** from intermediate **B** (Figure 3.11) is shown in Scheme 3.17.

Scheme 3.17

[65] Fellman, W.; Kaesz, H.D. *Inorg. Nucl. Chem. Lett.* **1966**, *2*, 63.
[66] Hoyano, J.K.; Graham, W.A.G. *Inorg. Chem.* **1972**, *11*, 1265.
[67] Yang, C.S.; Cheng, C.P.; Guo, L.W.; Wang, Y. *J. Chin. Chem. Soc.* **1985**, *32*, 17.

The fifth fraction obtained was light yellow in colour, and contained $[Re(CO)_5Cl]$. Once again, isolation of this product provides evidence in support of the formation of the $[Re(CO)_5]^-$ anion (ionic mechanism) or the $Re(CO)_5$ radical. Chlorine atom abstraction from solvent dichloromethane[58] or hydride substitution by chlorine[59] would afford the obtained rhenium pentacarbonyl chloro complex. Alternatively, labile chloride ions lost from the titanocene dichloride metalating agent could offer another source of the chlorine atom.

Fraction six yielded an orange coloured solid after separation and purification on the alumina column. Complex **30** was identified as the acyl compound $[Re(CO)_5\{C(O)Fc\}]$. The prevalence of the acyl intermediate **C** proposed earlier in Figure 3.11 is confirmed if one assumes the formation of **30** as being the product of acyl complex **C** and complexation of a carbonyl ligand. This acyl complex has previously been synthesized by Beck *et al.*[68] by reaction of $[CpFe(\eta^5-C_5H_4C(O)Cl]$ and $[Re(CO)_5]^-$ and structurally characterized. As before, cleaving of the Re-Re bond is observed. The Re-Re bond energy is far less than that of a Re-C(O) or Re-C(OEt)R bond, which again is lower than that of a Re-halide or Re-H bond.[60, 69] This can account for the ease of cleavage and formation of Re-Re bonds during reactions.

The target hexametallic biscarbene complex **33** *ax*, *eq*-[{μ-TiCp$_2$O$_2$-O,O'}{μ-Fe(C$_5$H$_4$)$_2$-C,C'}{CRe$_2$(CO)$_9$}$_2$] was eluted as a dark brown-red fraction, displaying a bridging ferrocene and titandioxy substituent between the two carbene ligands. X-ray diffraction studies elucidated the interesting variation in the substitution site of the bridging carbene ligand: on one end, axial substitution of the bridging carbene ligand on a Re$_2$(CO)$_9$-fragment, on the other, equatorial substitution. Steric constraints are assumed to be responsible for this unique substitution pattern, as the electronically favourable substitution site remains the equatorial site. As for the complexes synthesized in Chapter 2, the remaining chloro ligand of the titanoxy substituent displays enhanced activation and reacts with a second acylate oxygen to form **33**.

[68] Breimair, J.; Wieser, M.; Wagner, B.; Polborn, K.; Beck, W. *J. Organomet. Chem.* **1991**, *421*, 55.
[69] Elschenbroich, Ch.; Salzer, A. *Organometallics. An concise introduction* VCH Verlag, Weinheim, **1992**.

The eighth fraction was also deep red in colour. Although a very low yield (<5%) was obtained, the characterization of this complex could be achieved by NMR and IR spectroscopy, as well as mass spectrometry. Complex **32** *eq*-[$Re_2(CO)_9${C(OTiCp_2Cl)(Fc'CHO)}$]$ was identified, formed from a dilithiated ferrocene precursor, with reductive elimination of the $Re_2(CO)_9$-moiety only occurring on one side of the ferrocene, the other retaining its [$Re_2(CO)_9${C(OTiCp_2Cl)}$]$ metal carbene fragment. The same mechanism as proposed for the formation of FcCHO seems plausible in this case as well. Equatorial substitution of the carbene ligand was assigned from the IR spectrum of this compound. As has been observed from **31** and **33**, both equatorial (electronically favoured) and axial substitution (sterically favoured) are possible.

Finally, product nine was found to be the red monocarbene target complex **31**, *ax*-[$Re_2(CO)_9${C(OTiCp_2Cl)Fc}$]$. The assignment of an axial carbene ligand substitution was based purely on the infrared data obtained. This complex proved to be the least stable of the Fischer carbene metal cluster complexes. A summary of all the products obtained from this reaction is given in Figure 3.13.
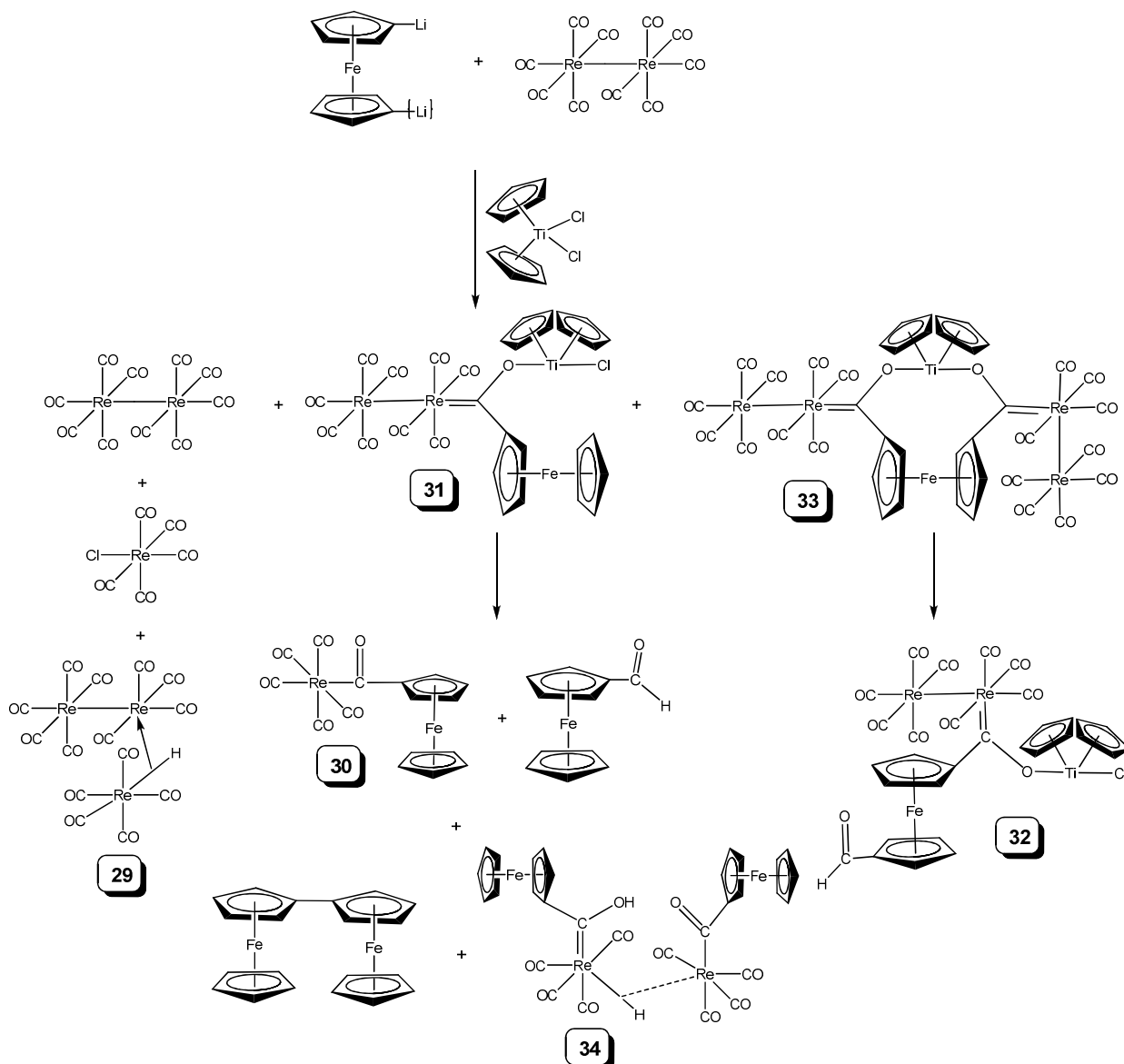
Figure 3.13   Fischer carbene transition metal complexes
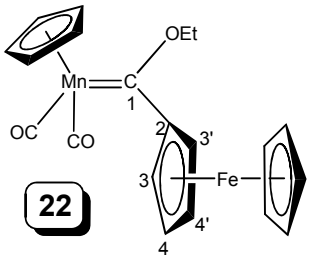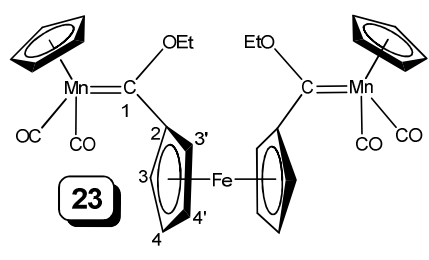
3.4   Spectroscopic characterization

The product compounds were characterized using ^{1}H and ^{13}C NMR and IR spectroscopy as well as mass spectrometry and the data confirmed the assigned structures. Further support of the molecular structures was found in solid state crystal structure determinations.

3.4.1   ^{1}H NMR spectroscopy

The proton NMR data of the manganese and rhenium complexes are listed in Tables 3.1 – 3.6, and the relevant numbering scheme employed are illustrated in each table respectively. The spectra of all the manganese carbene complexes were recorded in deuterated benzene as solvent, while chloroform-d[1] was employed for the rhenium complexes, with the exception of **30**. A spectrum of high quality could only be obtained in C_6D_6. Broadening of the signals of the manganese complexes **22** – **24** was observed. In the case of the rhenium complexes, slow decomposition of the products over time was observed.

Table 3. 1   ^{1}H NMR data of ethoxycarbene complexes of manganese
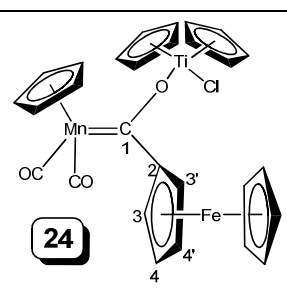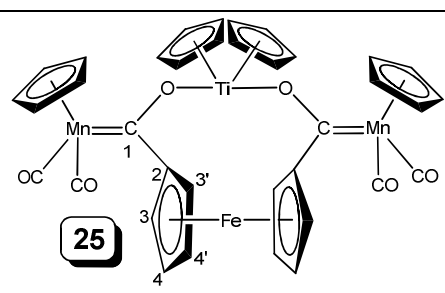
Proton Assignment	Chemical shifts (δ) and coupling constants (J)		
	δ*	δ*	J (Hz)
Mn-Cp	4.16, 5H, s	4.12, 10H, s	-
H3, H3'	4.83, 2H, br	4.92, 4H, dd	1.8, 1.8
H4, H4'	4.58, 2H, br	4.57, 4H, dd	2.0, 1.8
Fe-Cp	4.12, 5H, s	-	-
C**H**$_2$	4.80, 2H, br	4.82, 4H, q	7.0
C**H**$_3$	1.24, 3H, br	1.29, 6H, t	7.0

*   Recorded in C_6D_6

For the cyclopentadienyl manganese ferrocenyl carbene complexes, the biscarbene complexes show resonances consistently more downfield than that of the corresponding monocarbene complexes.

As seen for the Group VI transition metal carbene clusters, the H3, H3' α-proton of the ferrocenyl substituent gives a good indication of the electronic ring substituent involvement with the electrophilic carbene carbon atom, due both to its close proximity and the π-resonance effect, illustrated in Figure 2.15. Downfield shifts are observed in all cases, indicating the electron withdrawing effect of the metal carbonyl fragment bonded to the carbene ligand, as well as the π-delocalization of the ferrocene ring towards stabilizing the electrophilic carbene carbon atom.

Table 3.2 ^{1}H NMR data of titanoxycarbene complexes of manganese

Proton Assignment	Chemical shifts (δ) and coupling constants (J)		
	δ*	δ*	J (Hz)
Ti-Cp$_2$	6.20, 10H, s	6.37, 10H, s	-
Mn-Cp	4.03, 5H, s	4.38, 10H, s	-
H3, H3'	4.22, 2H, br	4.28, 4H, dd	1.7, 1.7
H4, H4'	3.87, 2H, br	3.99, 4H, dd	1.7, 1.7
Fe-Cp	4.19, 5H, s	-	-

*   Recorded in C$_6$D$_6$

If one employs the formula: Δδ = δ(H3, H3' of carbene complex) − δ(precursor ring proton), then a direct comparison can be made between carbene complexes containing the same [M(CO)$_n${C(Fc)}]-fragment to determine the

effect of the heteroatom carbene substituent (that is, the ethoxy substituent *vs* the titanoxy substituent on the carbene of the same metal). Alternatively, if the carbene ligand is kept constant, either {C(OEt)Fc} or {C(OTiCp$_2$Cl)Fc}, the effect of the central metal moiety on the electrophilic carbene carbon can be estimated (even if spectra were recorded in different deuterated solvents).

Table 3.3 ^{1}H NMR data of ethoxycarbene complexes of rhenium

Proton Assignment	Chemical shifts (δ) and coupling constants (J)				
	δ*†	J (Hz)	δ*	J (Hz)	δ*
H3$_{a,b}$, H3$_{a,b}$'	4.92, 2H, dd / *4.91, 2H, dd*	2.2, 1.8 / 2.2, 2.0	4.88, 4H, dd	3.9, 2.0	4.78, 4H, br
H4$_{eq}$, H4$_{eq}$' / H4$_{ax}$, H4$_{ax}$'	4.75, 2H, dd / *4.66, 2H, dd*	2.2, 2.2 / *1.9, 1.9*	4.63, 4H, dd	3.9, 2.0	4.68, 4H, br
Fe-Cp$_{eq}$ / *Fe-Cp$_{ax}$*	4.24, 5H, s / *4.27, 5H, s*	-	-	-	4.39, 10H, s
CH$_{2eq}$ / *CH$_{2ax}$*	4.67, 2H, q / *4.55, 2H, q*	6.7 / *7.2*	4.50, 4H, q	7.1	4.29, 4H, br
CH$_{3ax, eq}$	1.64, 6H, t (overlap)	6.9	1.69, 6H, t	6.9	1.53, 6H, br

*   Recorded in CDCl$_3$
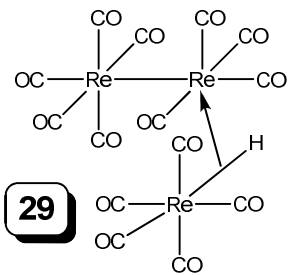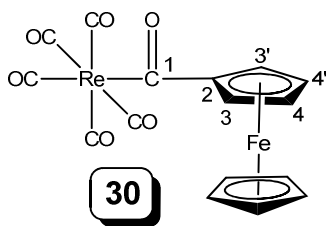†   Signal duplication is ascribed to the presence of both axial and equatorial isomers in solution

As seen from Tables 3.1 and 3.2, when the ethoxy substituent of the cyclopentadienyl manganese ethoxycarbene complexes is replaced by a titanoxy substituent, the chemical shift of the H3,3' proton is shifted upfield (compare for example **22,** Δδ = 0.79 while the titanoxy analogue **24** has Δδ =

0.18, and **23** has $\Delta\delta$ = 0.88 while $\Delta\delta$ = 0.24 for **25**). As for the Group VI ferrocenyl carbene, this indicates the greater electron donating power, or at least stabilization towards carbene carbon atom, of the titanoxy substituent compared to the ethoxy group. This is rationalized by the predominant acyl character of the C-O bond, and the ionic nature of the Ti-O bond, as shown previously in Figure 2.16.

Table 3. 4 ^{1}H NMR data of byproduct rhenium complexes

Proton Assignment	Chemical shifts (δ) and coupling constants (J)		
	δ*	δ**	J (Hz)
H3, H3'	-	4.49, 2H, dd	2.7, 2.4
H4, H4'	-	4.04, 2H, dd	2.7, 2.8
Fe-Cp	-	3.85, 5H, s	-
Re-H	-15.41, 1H, s	-	-

*   Recorded in $CDCl_3$
**   Recorded in C_6D_6

Duplication of all the chemical shifts is observed for complex **26** (Figure 3.14). In solution, both the axial and equatorial isomers are present in a ratio of approximately 1:1. Two-dimensional NMR experiments were used to distinguish between the two sets of signals, as listed in Table 3.3. It is anticipated that the carbene in the axial position will have the Re-atom more involved in π-backbonding because of poor π-interaction with the second Re-metal (Re-Re bond). As a result, less electron donation is expected from the Fc ligand and upfield resonances for H3 and H4, compared to the equatorial isomer, is expected. The remote ethoxy CH_3-group is hardly influenced, and only one
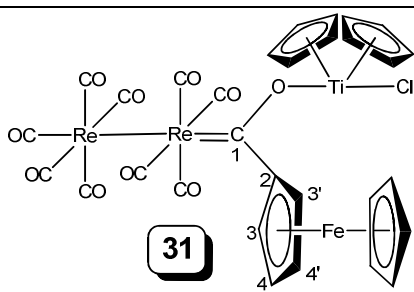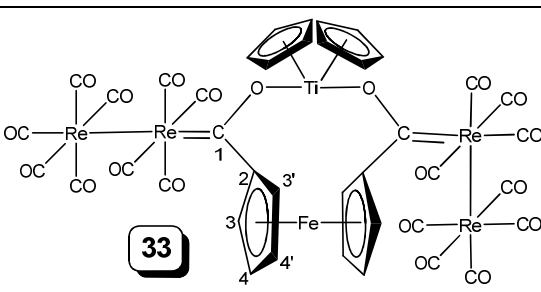
triplet is observed; however integration of the signal confirmed the resonance as that of six hydrogens, therefore two CH_3-groups.
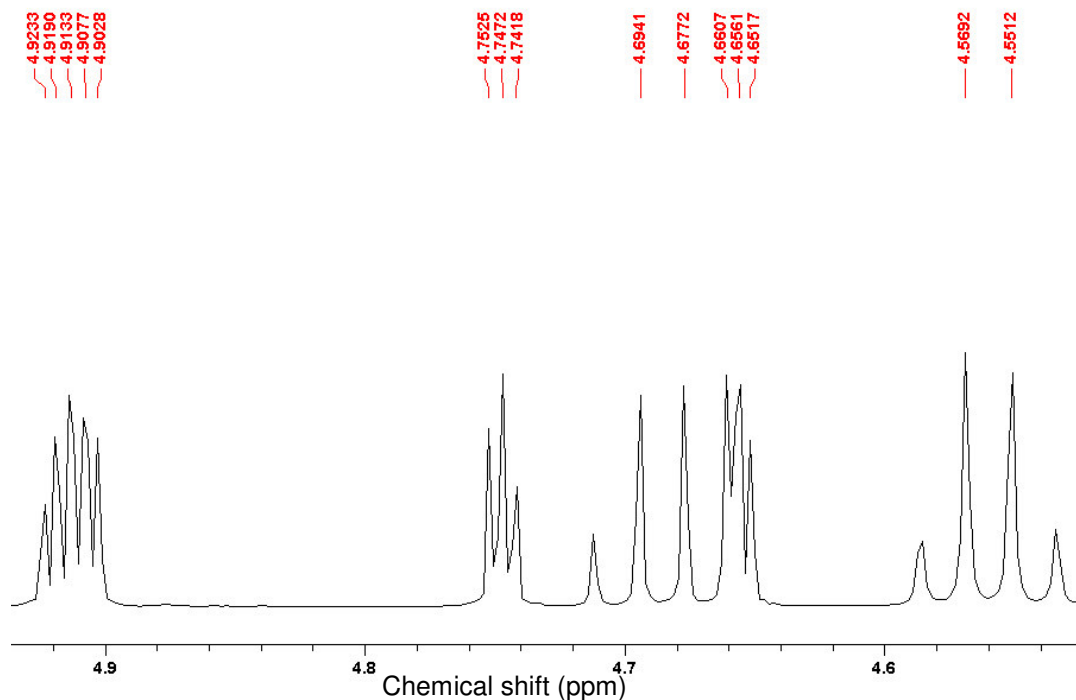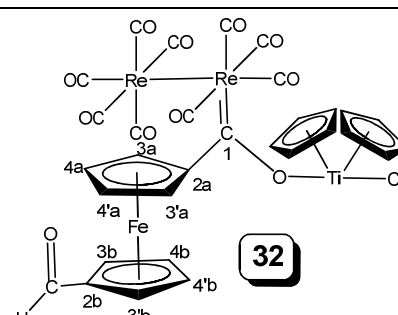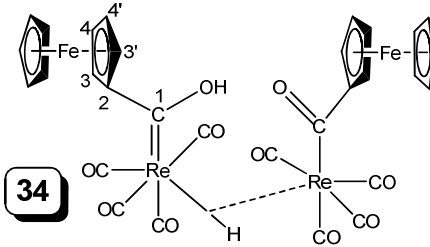
Figure 3.14   Excerpt of the ^{1}H NMR spectrum of **26** displaying presence of both equatorial and axial isomers in solution

Table 3.5 ^{1}H NMR data of titanoxycarbene complexes of rhenium

Proton Assignment	Chemical shifts (δ) and coupling constants (J)	
	31	**33**
	δ*	δ*
Ti-Cp$_2$	6.57, 10H, s	6.71, 10H, s
H3, H3'	4.98, 2H, br	4.97, 4H, br
H4, H4'	4.71, 2H, br	4.76, 4H, br
Fe-Cp	4.39, 5H, s	-

Table 3. 6   ^{1}H NMR data of byproduct rhenium carbene complexes

Proton Assignment	Chemical shifts (δ) and coupling constants (J)	
	δ*	δ*
C**H**O	9.97, 1H, s	-
C(O**H**)	-	9.93, 1H, s
Ti-Cp$_2$	6.56, 10H, s	-
H3$_a$, H3$_a$' / *H3$_b$, H3$_b$'*	4.91, 2H, br / *4.78, 2H, br*	5.03, 4H, br
H4$_a$, H4$_a$' / *H4$_b$, H4$_b$'*	4.71, 2H, br / *4.60, 2H, br*	4.98, 4H, br
Fe-Cp		4.70, 10H, br
Re-H		-15.59, 1H, s

*   Recorded in CDCl$_3$

For the two ferrocenyl ethoxycarbene rhenium complexes (*mono*-**26** and *bis*-**27**, the chemical resonances of the H3,3' protons are very similar, resulting in close values for Δδ: 0.72 and 0.69 ppm respectively. However, the bridged bischloro ferrocenyl biscarbene **28** contains an X-μ-L type ligand[7] for each metal centre, resulting in greater electron density available on the metal centres for backdonation towards the carbene carbon atom. This cascade effect results in less involvement of the ferrrocenyl rings towards carbene stabilization, and a resultant higher field chemical shift of the α-prontons.

If the carbene ligand is kept constant for comparison, all of the different metal moieties can be listed in order of electron donating power,[22] as illustrated in Figure 3.15. The cyclopentadienyl manganese group is proven to have the greatest π-electron donor strength, while the dirhenium nonacarbonyl fragment is the strongest electron withdrawing group.

$(OC)_2CpMn$=C, O-TiCp$_2$-O, Fc, C=MnCp(CO)$_2$ **25** $\Delta\delta = 0.24$ ppm

$(OC)_5Mo$=C, O-TiCp$_2$-O, Fc, C=Mo(CO)$_5$ **10** $\Delta\delta = 0.48$ ppm

$(OC)_5Cr$=C, O-TiCp$_2$-O, Fc, C=Cr(CO)$_5$ **8** $\Delta\delta = 0.51$ ppm

$(OC)_5W$=C, O-TiCp$_2$-O, Fc, C=W(CO)$_5$ **9** $\Delta\delta = 0.55$ ppm

$(OC)_9Re_2$=C, O-TiCp$_2$-O, Fc, C=Re$_2$(CO)$_9$ **33** $\Delta\delta = 0.78$ ppm

Increasing π-electron donor strength

$\Delta\delta = \delta(H3,H3'$ of carbene complex$) - \delta($precursor ring proton$)$
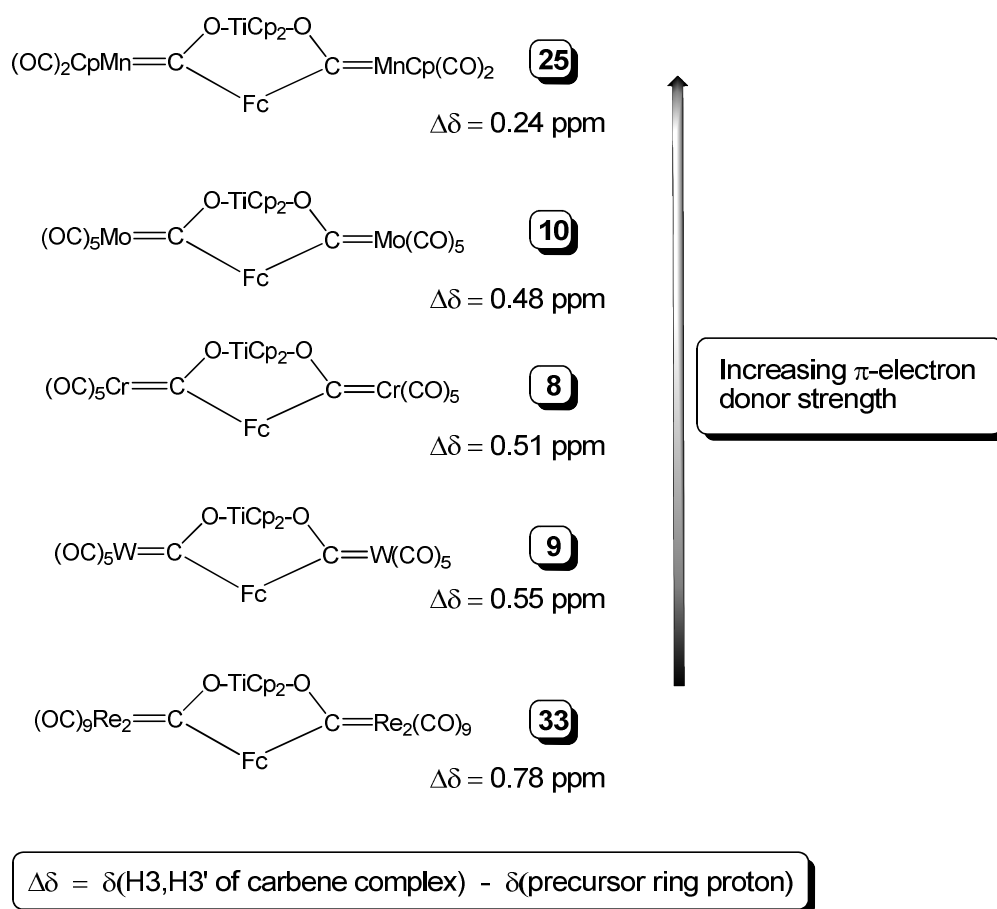
Figure 3.15 Central metal moiety effect on the carbene ligand

Table 3.6 lists the data of the two modified rhenium carbene complexes, **32** and **34**. In both cases, greater downfield shifts of H3,3' are observed than in any other case. Specifically for the acyl-hydrido hydroxycarbene complex **34**, the carbene heteroatom substituent cannot contribute towards π-stabilization of the

carbene, therefore much greater influence is felt on the ferrocenyl ring, and a Δδ-value of 0.99 is calculated for this complex.

Complex **34** is unusual in that it exhibits a hydroxycarbene trapped in a dinuclear acyl-hydroxycarbene, and also displays a bridging rhenium hydride. The two most significant signals in the spectrum are the highfield and lowfield signals that correspond to the hydridic and the protonic hydrogen atoms of the complex. The peak at 9.93 ppm is assigned to the protonic hydrogen. This hydrogen atom is, however, not as deshielded as that of the analogous thienyl acyl-hydrido/hydroxycarbene prepared by Olivier.[31] For the thienyl acyl hydroxycarbene, a singlet at δ: 21.5 was assigned to the protonic hydrogen. In the case of the Shvo catalyst (Figure 3.7), better agreement was found with the value obtained in this study, where the Shvo proton displays a chemical shift of around 8 ppm[49] compared to the value of 9.93 ppm found for the ferrocenyl acyl-hydrido hydroxycarbene. This could indicate that the protonic hydrogen of **34** is not O-H-O bridging, possibly due to steric reasons, so that a conformation of **34** where the acyl fragment is twisted to the opposite side of the hydroxycarbene ligand is found. As speculated in Scheme 3.18, the resulting weaker link between the two Re-fragments, and the orientation of the bridging hydride and acyl would assist in aldehyde elimination/decomposition. The bridging hydride value of -15.59 ppm is also in good agreement with the values obtained for the corresponding thienyl complex (δ: -15.7) and the Shvo catalyst (δ: -17.9).
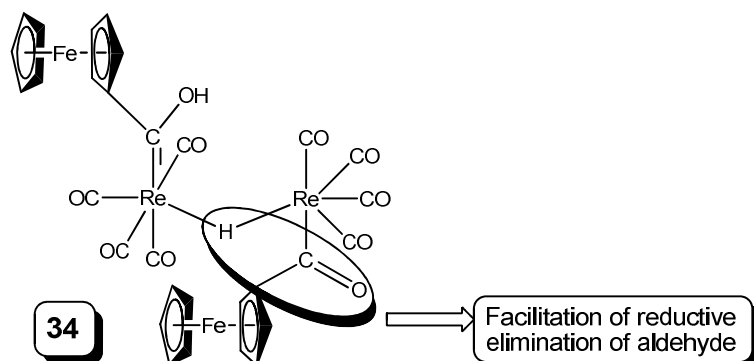
Scheme 3.18

It is interesting to note that complex **34** appears to have a symmetrical structure at room temperature in solution, as the signals for the two ferrocenyl ligands coincide. Therefore the two constituent parts lose their individual identity, and two resonance structures can be drawn to support this statement as the extended double bond character of the Re-C(carbene) and C(carbene)-O bonds in Scheme 3.19 demonstrates. However, this factor disputes the speculation on the opposite orientation of the hydroxycarbene and acyl ligands.
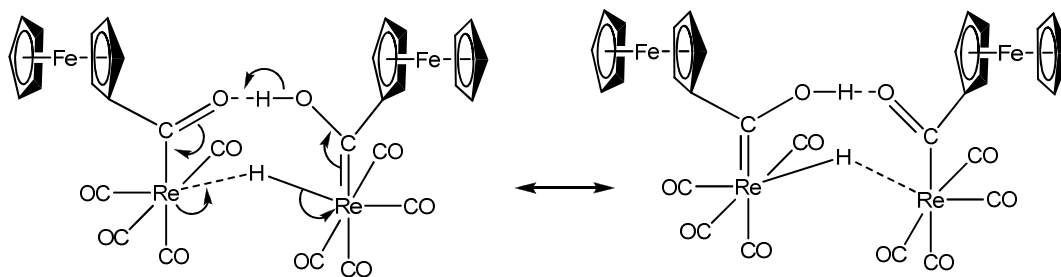
Scheme 3.19

3.4.2 ^{13}C NMR spectroscopy

The ^{13}C NMR data for the manganese complexes are summarized in Tables 3.7 and 3.8, while the data of the rhenium complexes are listed in Tables 3.9 – 3.12. The same atom numbering scheme is used as for the ^{1}H NMR spectra in Section 3.4.1.

Table 3.7 ^{13}C NMR data of ethoxycarbene complexes of manganese

Carbon Assignment	Chemical shifts (δ)	
	22	**23**
	δ*	δ*
C1	328.5	336.5
Mn-CO	232.0, 230.4	231.9
C2	95.9	96.5
Mn-Cp	83.8	84.0
C3, C3'	73.6	73.9
C4, C4'	72.3	72.3
Fe-Cp	71.3	-
CH$_2$	73.7	74.7
CH$_3$	14.8	15.3

*   Recorded in C$_6$D$_6$

Table 3.8 ^{13}C NMR data of titanoxycarbene complexes of manganese

Carbon Assignment	Chemical shifts (δ)	
	24	**25**
	δ*	δ*
C1	321.8	338.4
Mn-CO	n.o.	233.7
Ti-Cp$_2$	118.2	117.7
C2	n.o.	n.o.
Mn-Cp	82.7	85.7
C3, C3'	71.3	69.3
C4, C4'	70.1	68.2
Fe-Cp	64.2	-

*   Recorded in C$_6$D$_6$

The carbene carbon resonances of the cyclopentadienyl manganese complexes fall well within the range expected for CpMn-carbene complexes.[70] As in the proton NMR spectra, the biscarbene complexes' chemical resonances are consistently lower field than the corresponding monocarbene complexes. Especially prominent are the carbene carbon chemical shifts, which show differences of 8 – 17 ppm. This downfield shift of the biscarbene carbon resonance compared to the monocarbene resonance is not observed for the rhenium complexes.

Table 3.9 ^{13}C NMR data of ethoxycarbene complexes of rhenium

Carbon Assignment	Chemical shifts (δ) and coupling constants (J)		
	26	**27**	**28**
	δ*†	δ*	δ *
C1$_{eq}$	306.3	307.7	n.o.
C1$_{ax}$	275.6		
Re-CO$_{eq, ax}$ (overlap)	199.2, 199.1, 194.9, 193.1, 189.7	198.8, 194.6, 192.3, 189.2	199.2, 191.9
C2$_{eq}$	98.8	102.0	n.o.
C2$_{ax}$	96.1		
C3$_{eq}$ C3$_{ax}$'	n.o. (overlap solvent signal)	74.7	74.0
C4$_{eq}$	73.2	72.8	71.8
C4$_{ax}$'	72.6		
Fe-Cp$_{eq}$	70.7	-	70.7
Fe-Cp$_{ax}$'	70.4		
CH$_{2eq}$	76.3	77.8	76.3
CH$_{2ax}$	74.0		
CH$_{3eq, ax}$ (overlap)	14.8	14.8	14.8

*   Recorded in CDCl$_3$
†   Signal duplication is ascribed to the presence of both axial and equatorial isomers in solution

---

[70] Mann, B.E. *Adv. Organomet. Chem.* **1974**, *12*, 135.

The titanium Cp-rings in the manganese monocarbene complex **24** rotate freely in solution, as is evident from a single peak for the Cp-protons as well as carbon atoms in the NMR spectra, while the ^{13}C NMR spectrum of the ferrocenyl monocarbene rhenium complexes **31** and **32** display two signals. This observation is ascribed to restricted rotation of the C(carbene)-C(Fc) bond caused by the proximity of the bulky metal substituents. For the biscarbene complexes **25** and **33**, the symmetry of the structures precludes electronic inequivalency and only one titanium Cp-resonance is seen.

Table 3.10 ^{13}C NMR data of byproduct rhenium complexes

Carbon Assignment	Chemical shifts (δ)	
	29	**30**
	δ*	δ*
C1	-	234.8
Re-CO	196.1, 190.6 (*ax*-(CO)$_9$) 186.5, 186.3, 178.9 (*eq*-(CO)$_9$) 183.6 (*cis*-(CO)$_5$) 176.8 (*trans*-(CO)$_5$)	191.9, 183.9, 181.6
C2	-	n.o.
C3, C3'	-	80.4
C4, C4'	-	72.7
Fe-Cp	-	69.7

*   Recorded in CDCl$_3$

Well-resolved carbonyl signals were observed for **29**. The downfield resonances are assigned to the less shielded Re$_2$(CO)$_9$-fragment, while the Re(CO)$_4$H-fragment display two resonances more upfield. The carbonyl *trans* to the hydride ligand receives more π-electron backdonation from the metal, and is therefore assigned the highest field signal, while competition between two π-accepting CO ligands *trans* to each other leads to less shielding, and a downfield shift of the *cis*-CO ligands of the Re(CO)$_4$-group.

When comparing the carbene carbon resonances of the ethoxycarbene complexes (**26**, **27**) with those of the titanoxycarbene carbons (**32**, **33**), a clear upfield shift of the titanoxy analogues would seem to support the finding that the titanoxy fragment better stabilizes the carbene carbon atom than an ethoxy group (similarly to the results obtained form proton NMR spectra and the comparison of the H3,3' chemical shifts).

Table 3.11 ^{13}C NMR data of titanoxycarbene complexes of rhenium

Carbon Assignment	Chemical shifts (δ)	
	31	**33**
	δ*	δ*
C1	n.o.	272.6
Re-CO	178.9, 176.9	199.8, 193.8, 192.5, 186.9, 186.3, 186.2
Ti-Cp$_2$	120.1, 118.9	125.8
C2	85.1	95.5
C3, C3'	76.3	74.1
C4, C4'	71.5	72.2
Fe-Cp	70.5	-

*   Recorded in CDCl$_3$

The ^{13}C NMR spectrum of **26** displays duplication of the signals similar to that observed in the ^{1}H NMR spectrum (Figure 3.14). Similarly to the proton spectrum, a tentative assignment of the axial and equatorial isomers can be made. For the equatorially substituted complex, the carbene ligand would be *trans* to the greater π-acceptor group, a carbonyl ligand, and would therefore be less shielded and the carbene carbon would resonate more downfield. For an axially substituted carbene complex, the group *trans* to the carbene ligand would be the Re(CO)$_5$-fragment, an X-type ligand. The isomer with carbene carbon δ:

306.3, can therefore be assumed to be the equatorial carbene complex, and the other isomer (carbene carbon δ: 275.6) as the axial isomer.

Complex **30** contains an acyl functionality, where the C=O chemical shift occurs at 234.8 ppm. In contrast, the most downfield carbene carbon atom resonance, 307.7 ppm, is that of complex **27**, the bisethoxycarbene complex. An intermediate value of 272.6 ppm is observed for the titanoxy biscarbene complex **33**. For the acyl-hydrido hydroxycarbene complex **34**, both the acyl (δ: 231.5) and the extremely downfield hydroxycarbene signal (δ: 346.2) are observed. The observation of these separate resonances would indicate that doubt about the presence of the bridging O-H-O hydrogen bond in solution is justified, and supports the speculated arrangement given in Scheme 3.18. In contrast, the ferrocenyl and carbonyl signals coincide as for a symmetrical system (observed in the ^{1}H NMR system, as well as for the acyl hydroxycarbene of Olivier[31]).

Table 3.12   ^{13}C NMR data of byproduct carbene complexes of rhenium

Carbon Assignment	Chemical shifts (δ)	
	32	**34**
	δ*	δ*
C1	287.0	346.2, 231.5
Re-CO	200.9, 195.7	185.9
CHO	178.9	
Ti-Cp$_2$	120.2, 119.2	-
C2	n.o.	n.o.
C3$_{a,b}$, C3'$_{a,b}$	74.5, 73.2	76.0
C4$_{a,b}$, C4'$_{a,b}$	71.3, 69.6	74.0
Fe-Cp	-	70.8

* Recorded in CDCl$_3$

3.4.3   IR spectroscopy

The number and intensities of carbonyl stretching frequencies are dependent on the local symmetry of the carbonyl ligands around the central atom. The IR spectra of the carbonyl vibration of cyclopentadienyl manganese mono- and biscarbene complexes show two bands: the IR-active $\upsilon(CO)$ A_1 and B_1 band. The A_1 band occurs at higher frequency, but the bands have roughly equal intensity.[71]

The infrared data (recorded in dichloromethane) of the manganese complexes are summarized in Table 3.13. Complex **24** decomposed during measurement, and no resolved spectrum of this compound could be obtained.

As expected, the ethoxycarbene complexes displayed carbonyl stretching vibrations at higher frequencies, implying stronger Mn-C(carbene) backbonding compared to the titanoxycarbene **25**.

Table 3.13   Infrared data of manganese cluster carbene complexes

| Complex	$MCp(CO)_2$ assignment, $[\upsilon(CO), cm^{-1}]$*	
	A_1	B_1
22	1938 vs	1862 s
23	1927 vs	1858 s
25	1922 vs	1849 s

*   Spectra recorded in CH_2Cl_2

The carbonyl stretching modes of equatorially and axially substituted bimetal nonacarbonyl complexes were summarized by Ziegler *et al.*[72] The *eq*-$[M_2(CO)_9L]$ displays a nine band pattern in the IR spectrum, corresponding to C_s symmetry (Figure 3.16). These bands include six A' bands and three degenerate A'' bands. On the other hands, the IR spectrum of *ax*-$[M_2(CO)_9L]$ is observed to
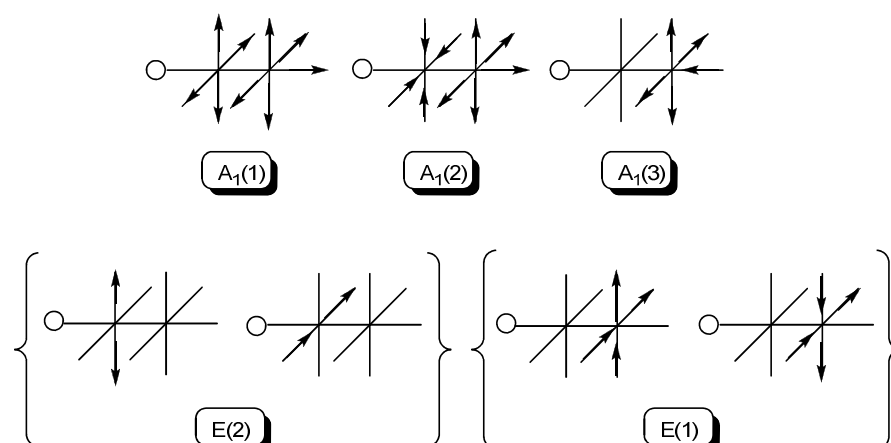
---

[71] Adams, D.M. *Metal-Ligand and Related Vibrations,* Edward Arnold Publishers Ltd., London, **1967**, 98.
[72] Ziegler, M.L.; Haas, H.; Sheline, R.K. *Chem. Ber.* **1965**, *98,* 2454.

have only five bands: three A' bands and two E bands, according to C_{4v} symmetry (Figure 3.17).
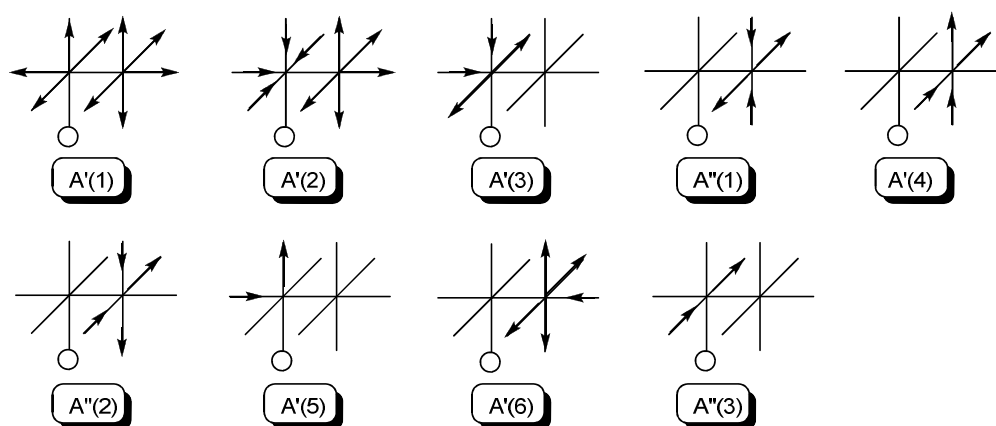
Figure 3.16   IR-active normal modes observed for eq-[$M_2(CO)_9L$]

Figure 3.17   IR-active normal modes observed for ax-[$M_2(CO)_9L$]

Due to the low solubility of the rhenium complexes in the nonpolar solvent hexane, the IR spectra of all complexes were recorded in dichloromethane. Dichloromethane does not have the same resolution power as hexane, and results in both lifting of band degeneracy in DCM, and a great extent of band overlap. Assignment of the carbonyl bands were therefore considerably complicated, and no clear distinction between the equatorial and axial isomers could be made. Instead, the observed bands are listed in Table 3.14.

Table 3.14   Infrared data of octahedral dirhenium nonacarbonyl complexes

Complex	Carbonyl stretching frequencies (cm^{-1})*
26	Mixture: eq-$M_2(CO)_9$ and ax-$M_2(CO)_9$ Overlapping bands: 2101 w, 2039 m, 1996 vs, 1970 m, 1938 m
27	eq-$M_2(CO)_9$ Overlapping bands: 2102 m, 2038 m, 1995 vs, 1968 sh, 1940 m
28	fac-$M(CO)_3$, from precursor cis-$M(CO)_4$ 2101 m (A_1^1), 2036 m (A_1^2), 1991 s (B_1), 1936 m (B_2)
29	Combination: eq-$M_2(CO)_9$ and $M(CO)_5$ Overlapping bands: 2147 w, 2101 s, 2046 vs, 2016 m, 1989 vs, 1922 m
30	$M(CO)_5$ 2140 m (A_1^2), 2038 m (B_1), 2010 s (A_1^1), 1975 vs (E), 1565 m (acyl)
31	ax-$M_2(CO)_9$ 2156 w (A_1^1), 2064 w (A_1^2), 2046 vs(E_1), 1985 s (A_1^3), 1929 m (E_2)
32	eq-$M_2(CO)_9$ Overlapping bands: 2099 w, 2046 m, 2023 m, 1988 vs, 1953 m, 1917 s, 1883 w, 1684 w (CHO)
33	Combination: eq-$M_2(CO)_9$ and ax-$M_2(CO)_9$ Overlapping bands: 2098 m, 2084 w, 2046 vw, 2027 m, 2005 s, 1991 vs, 1958 m, 1933 m, 1919 m
34	Two different systems of cis-$M(CO)_4$ 2083 w(A_1^2, 2069 w (A_1^2, 2012 vs (B_1), 1985 sh (B_1) 1971 m (A_1^1), 1955 m (A_1^1), 1926 w (overlap, B_2), 1610 w (acyl)

*   Spectra recorded in CH_2Cl_2

For **26** (a mixture of equatorial and axial $M_2(CO)_9$-systems), **27** (*eq*-$M_2(CO)_9$), **29** (a combination of an *eq*-$M_2(CO)_9$ and an $M(CO)_5$-system), **32** (*eq*-$M_2(CO)_9$) and **33** (a combination of an *eq*-$M_2(CO)_9$ and an *ax*-$M_2(CO)_9$-system), band overlap prevented band assignment. The facially substituted, octahedral $M(CO)_3$-system of complex **28** resulted in four νCO bands. For a *fac*-$M(CO)_3L_3$ octahedral complex, two IR active bands are expected, namely the A_1 band (at higher frequency) and the E band, roughly twice the intensity of the A_1 band as well as broader, due to partial lifting of the degeneracy by asymmetric ligands.[71] This pattern was not obtained. Instead, the four bands displayed the pattern expected for a *cis*-$M(CO)_4L_2$ system, containing two A_1 bands, a B_1 and a B_2 band that are IR active. This was ascribed to the precursor *cis*-[Re(CO)$_4${C(OEt)Fc}Cl] that is present during the formation of **28**, as depicted in Scheme 3.13.

For complex **30**, the expected $M(CO)_5L$-pattern of four bands for pseudo-C_{4v} symmetry is obtained, in good agreement with literature values.[68] However, literature records the presence of two acyl bands at 1572 and 1543 cm^{-1}, while only one band at 1565 cm^{-1} was observed in this study.
The five νCO bands corresponding to *ax*-$M_2(CO)_9L$ was observed for **31**.

Acyl hydrido hydroxycarbene **34** displayed a duplication of signals, similarly to that of **28**. A *cis*-$M(CO)_4L$ system should display four IR active bands; two A_1 bands, a B_1 and a B_2 band. The signal duplication would seem to support the finding of a non-symmetrical structure of **34**, precluding the presence of an O-H-O bridge. Further support of this comes from the presence of the distinct acyl C-O stretching frequency at 1610 cm^{-1}, therefore the speculated arrangement of **34** in Scheme 3.18, rather than the orientation suggested in Scheme 3.19, seems more plausible.
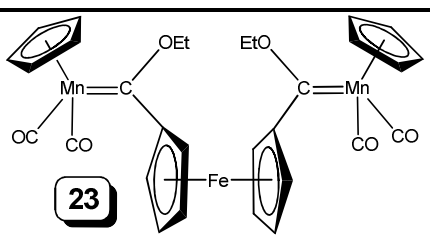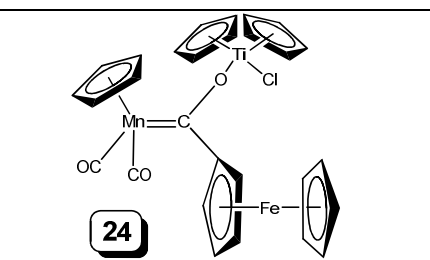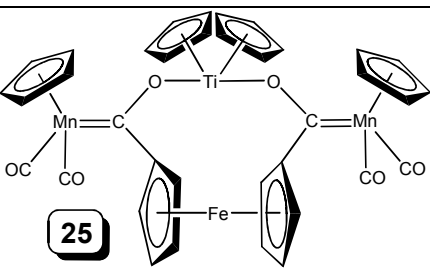
3.4.4 Mass spectrometry

FAB-MS methods in a 3-nitrobenzyl alcohol matrix were employed to record the mass spectra of the manganese carbene complexes **23** – **25**, and the mass

spectral data are summarized in Table 3.15. No molecular ion peak (M^+), nor any other m/z peak could be identified for **22**.

Limited information could be obtained from the mass spectral data listed below. The molecular ion peak was identified in all three cases, as well as the peak representing the fragment ion after loss of two carbonyl ligands, evidence of correct structure assignment. For both **23** and **24**, loss of the heteroatom carbene substituent was observed as well. Connor *et al.* reported a novel metal-extrusion process for the $[Mn(MeCp)(CO)_2\{C(OMe)Fc\}]$ complex where the ion $[Mn(MeCp)Fc]^+$ lost manganese to give $[MeCpFc]^+$ as well as the dimerisation product olefin, $[Fc\{C(OEt)\}]_2$.[22] None of these peaks could be identified during this study.

Table 3.15   Mass spectral data of manganese carbene complexes

Complex	m/z	Intensity (%)	Fragment Ion
23	650	3.5	$[M]^+$
	594	4.2	$[M - 2CO]^+$
	577	2.8	$[M - CO - OEt]^+$
24	603	1.5	$[M]^+$
	511	2.0	$[M - 2CO - Cl]^+$ or $[M - CO - Cp]^+$
	389	15.0	$[M - TiCp_2Cl]^+$
25	770	1.1	$[M]^+$
	714	0.8	$[M - 2CO]^+$

No mass spectrum could be obtained for complex **30**, and no M^+ molecular ion peaks were observed for complexes **28** and **33**. The mass spectral data of all rhenium complexes barring that of **30** are listed in Table 3.16.

Stepwise fragmentation of the carbonyl ligands, followed by loss of the terminal $Re(CO)_5$-fragments were observed consistently for all of the rhenium complexes (Figure 3.18). For the ethoxycarbene complexes, loss of the carbene substituents (either the ferrocenyl or ethoxy substituents) did not feature in the fragmentation pattern, although the bridged dichloro biscarbene complex **28** did display loss of the bridging chloro ligands.
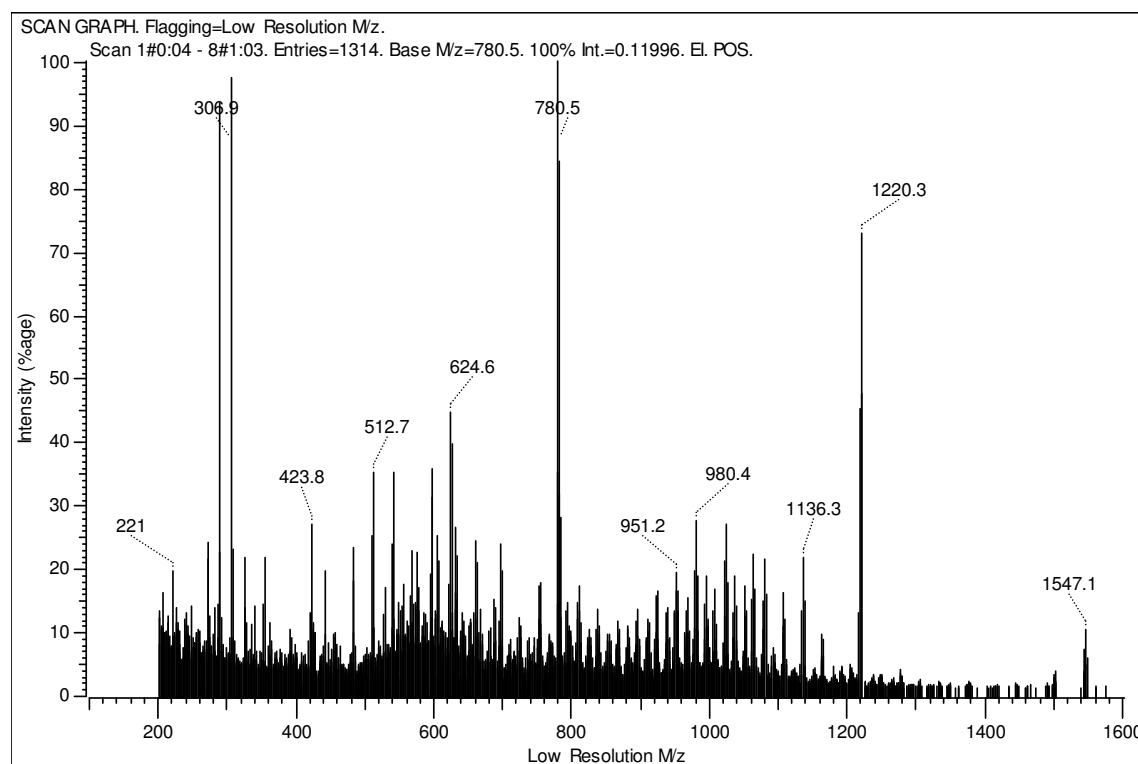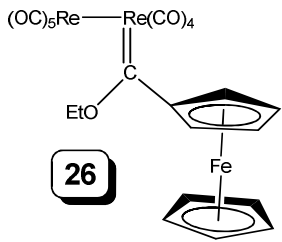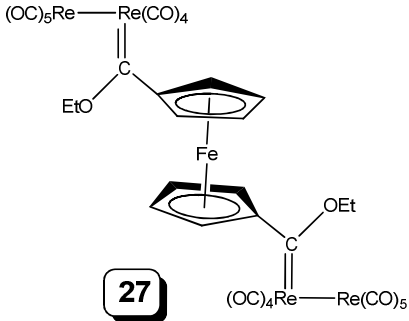

Figure 3.18　　　Stepwise loss of CO ligands, followed by subsequent loss of $Re(CO)_5$-units in the mass spectrum of complex **27**

In contrast, the mass spectra of the titanoxycarbene rhenium complexes show loss of both titanocene (chloride) and ferrocenyl, to yield the corresponding acyl
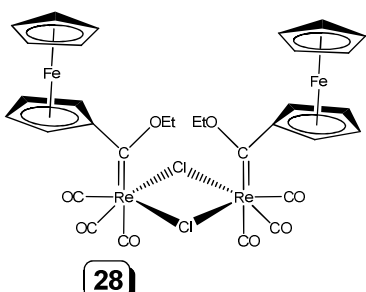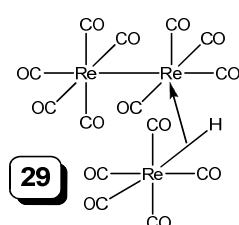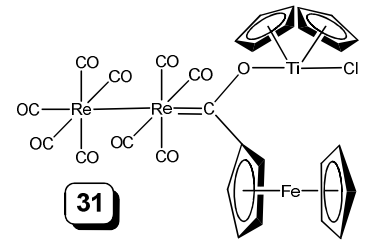
complexes. In some cases, loss of the entire carbene ligand was observed. The decomposition aldehyde (FcCHO) and dimerization product biferrocene were observed in the mass spectra of compounds **32** and **34** respectively, and re-formation of the precursor dirhenium decacarbonyl was seen for **34**.
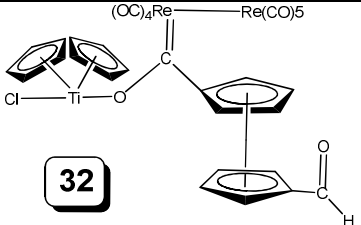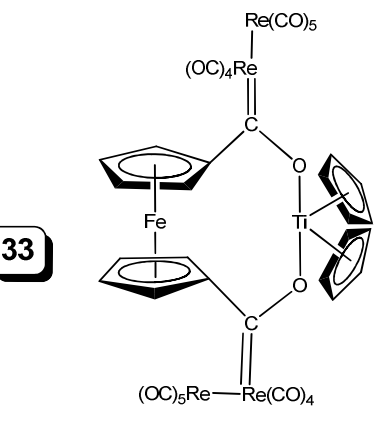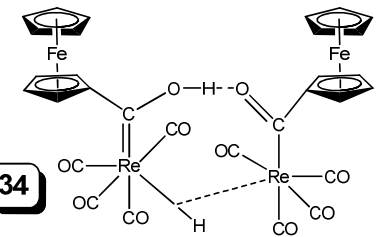
Table 3.16   Mass spectral data of rhenium complexes

Complex	m/z	Intensity (%)	Fragment Ion
26	867	1.7	$[M]^+$
	782	0.5	$[M - 3CO]^+$
	541	8.1	$[M - Re(CO)_5]^+$
	513	6.5	$[M - Re(CO)_5 - CO]^+$
	484	7.2	$[M - Re(CO)_5 - 2CO]^+$
27	1547	11	$[M]^+$
	1502	40	$[M - OEt]^+$
	1491	20	$[M - 2CO]^+$
	1220	75	$[M - Re(CO)_5]^+$
	1164	11	$[M - Re(CO)_5 - 2CO]^+$
	1136	22	$[M - Re(CO)_5 - 3CO]^+$
	1108	16	$[M - Re(CO)_5 - 4CO]^+$
	1080	22	$[M - Re(CO)_5 - 5CO]^+$
	1052	17	$[M - Re(CO)_5 - 6CO]^+$
	1024	27	$[M - Re(CO)_5 - 7CO]^+$
	980	28	$[M - 2Re(CO)_5]^+$
	952	19	$[M - 2Re(CO)_5 - CO]^+$
	867	14	$[M - 2Re(CO)_5 - 2CO]^+$
	811	13	$[M - 2Re(CO)_5 - 3CO]^+$
	781	10	$[M - 2Re(CO)_5 - 4 CO]^+$
	755	19	$[M - 2Re(CO)_5 - 5CO]^+$
	699	21	$[M - 2Re(CO)_5 - 7CO]^+$

Table 3.16 *contd. 2*   Mass spectral data of rhenium complexes

Complex	m/z	Intensity (%)	Fragment Ion
28	541	48	$[M - Re(CO)_3Cl\{C(OEt)\}\ -Cl]^+$
	513	32	$[M - Re(CO)_3Cl\{C(OEt)\} - Cl - CO]^+$
	485	42	$[M - Re(CO)_3Cl\{C(OEt)\} - Cl - 2CO]^+$
	457	12	$[M - Re(CO)_3Cl\{C(OEt)\} - Cl - 3CO]^+$
29	952	48	$[M]^+$
	811	7.5	$[M - 5CO]^+$
	783	6	$[M - 6CO - H]^+$
	625	100	$[Re_2(CO)_9]^+$
	598	62	$[M - Re(CO)_5H - CO]^+$
	569	16	$[M - Re(CO)_5H - 2CO]^+$
	542	5	$[M - Re(CO)_5H - 3CO]^+$
31	1052	0.7	$[M]^+$
	1015	0.5	$[M - Cl]^+$
	995	0.3	$[M - 2CO]^+$
	725	8.0	$[M - Re(CO)_5]^+$
	690	2.4	$[M - Re(CO)_5 - Cl]^+$
	653	2.4	$[M - TiCp_2Cl - Fc]^+$
	625	2.1	$[M - \{C(OTiCp_2Cl)Fc\}]^+$
	597	1.9	$[M - \{C(OTiCp_2Cl)Fc\} - CO]^+$
	512	6.0	$[M - \{C(OTiCp_2Cl)Fc\} - 4CO]^+$
	484	6.2	$[M - \{C(OTiCp_2Cl)Fc\} - 4CO]^+$

135

Table 3.16 *contd. 3*   Mass spectral data of rhenium complexes

Complex	m/z	Intensity (%)	Fragment Ion
32	1079	0.5	$[M]^+$
	753	39	$[M - Re(CO)_5]^+$
	540	4	$[M - Re(CO)_5 - TiCp_2Cl]^+$
	214	21	$[FcCHO]^+$
33	1014	1.9	$[M - 2Re(CO)_5]^+$
	986	2.1	$[M - 2Re(CO)_5 - CO]^+$
	930	1.9	$[M - 2Re(CO)_5 - 3CO]^+$
	904	1.2	$[M - 2Re(CO)_5 - 4CO]^+$
	874	1.2	$[M - 2Re(CO)_5 - 5CO]^+$
	838	2.8	$[Re_2(CO)_9\{C(O)Fc\}]^+$
	810	3.2	$[Re_2(CO)_9\{C(O)Fc\} - CO]^+$
	782	4.8	$[Re_2(CO)_9\{C(O)Fc\} - 2CO]^+$
	754	2.0	$[Re_2(CO)_9\{C(O)Fc\} - 3CO]^+$
	726	3.2	$[Re_2(CO)_9\{C(O)Fc\} - 4CO]^+$
	698	2.0	$[Re_2(CO)_9\{C(O)Fc\} - 5CO]^+$
	689	2.6	$[Re(CO)_4\{C(OTiCp_2)Fc\}]^+$
	653	15.7	$[Re_2(CO)_{10}]^+$
	625	10.4	$[Re_2(CO)_9]^+$
	597	10.6	$[Re_2(CO)_8]^+$
	569	3.8	$[Re_2(CO)_7]^+$
34	1022	0.8	$[M]^+$
	994	0.4	$[M - CO]^+$
	910	0.5	$[M - 4CO]^+$
	810	3.5	$[M - \{C(OH)Fc\}]^+$
	782	3.0	$[M - \{C(OH)Fc\} - CO]^+$
	726	1.2	$[M - \{C(OH)Fc\} - 3CO]^+$
	698	0.5	$[M - \{C(OH)Fc\} - 4CO]^+$
	370	95	$[Fc-Fc]^+$

The presence of a high intensity peak of the $[M - Re(CO)_5]^+$ fragment in all compounds containing a $Re_2(CO)_9$-moiety indicates the low bond strength of the Re-Re bond, as mentioned previously in the text.

3.4.5 Single crystal X-ray crystallography

Single crystals of suitable quality were obtained for complexes **23**, **27**, **28** and **33** and X-ray diffraction confirmed the molecular structures of these compounds. Layering of different ratios of dichloromethane/hexane was used as solvent from which the complexes crystallized. In the case of **28**, solvent inclusion during crystallization occurred, and equimolar amounts of dichloromethane co-crystallized with the complex molecules. ORTEP[73] + POV-Ray[74] drawings of the molecular structures are presented in Figures 3.19, 3.21 – 3.23, indicating the relevant atom numbering system employed. Experimental details are given in the experimental section and crystallographic data and refinement parameters are listed in the Appendices. Selected bond lengths, bond angles and torsion angles are given in Table 3.17 for the manganese biscarbene complex **23**, and the rhenium biscarbene complexes (**27**, **28** and **33**) in Tables 3.18 and 3.19.

3.4.5.1 Molecular structures

In the crystal structure of **23** (Figure 3.19), the space occupied by the two ethoxy groups, which lie one above the other, is similar to that occupied by the ferrocenyl group. Thus one enantiomer of the complex can occupy the crystal space of the other enantiomer with three carbon atoms of each Cp ring nearly coinciding with the non-hydrogen atom positions of the two ethyl groups. Therefore the crystal structure is disordered with 8(2)% of the other enantiomer occupying the site of each molecule. The minor position occupied by the iron

---

[73] Farrugia, L.J. *J. Appl. Crystallogr.* **1997**, *30*, 565.
[74] The POV-Ray Team, POV-Ray 2004. URL: http://www. povray.org/download/.

atom and the four carbon atom positions needed to complete the two Cp rings are shown as small spheres in Figure 3.19.

The molecule has approximate C_2 symmetry and thus the corresponding bond lengths, bond angles, and torsion angles surrounding the two carbene carbon atoms are approximately equivalent, therefore discussion of the structure will focus on only the Mn(1)-terminal half of the molecule.
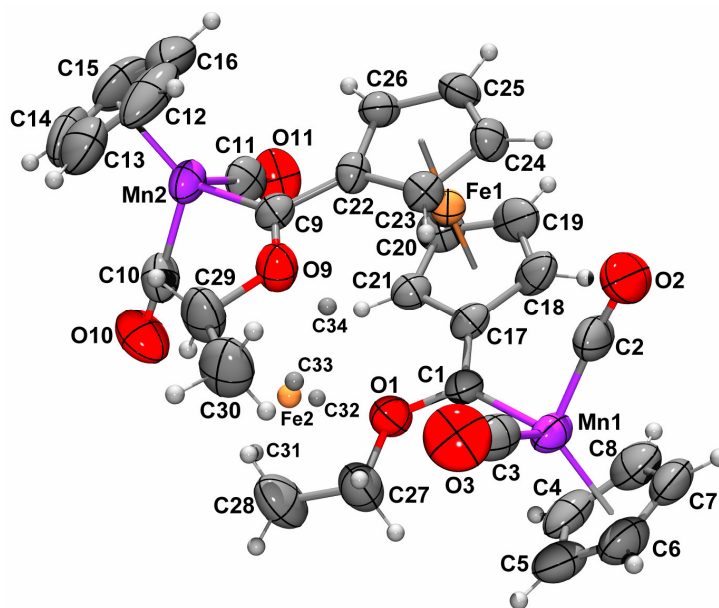
Figure 3.19   ORTEP + POV-Ray drawing of the molecular structure of **23**. Atomic displacement ellipsoids are shown at the 50% probability level.

In [MnCp(CO)$_2${C(OR)Y}] complexes, with two different organic substituents R and Y (Y = planar ring substituent), there are three possible conformations (**I**, **II** and **III** in Figure 3.20) as far as the mutual orientation of the carbene plane and the MnCp(CO)$_2$-moiety is concerned. In **I**, the carbene plane is perpendicular to the mirror plane of the MnCp(CO)$_2$ fragment with C_s symmetry. In both **II** and **III**, the carbene plane coincides with the mirror plane, but different positions of the organic substituents are assumed.

Table 3.17   Selected bond lengths (Å), bond angles (°) and torsion angles (°) for **23**

Bond lengths		Bond angles	
Mn(1)-C(1)	1.924(5)	Mn(1)-C(1)-O(1)	127.1(3)
Mn(2)-C(9)	1.916(5)	Mn(2)-C(9)-O(9)	128.7(3)
C(1)-O(1)	1.340(5)	Mn(1)-C(9)-C(17)	126.3(3)
C(9)-O(9)	1.338(5)	Mn(2)-C(9)-C(22)	126.4(3)
C(1)-C(17)	1.447(6)	O(1)-C(1)-C(17)	106.3(4)
C(9)-C(22)	1.446(6)	O(9)-C(9)-C(22)	104.4(4)
O(1)-C(27)	1.439(5)	C(1)-O(1)—C(27)	123.1(4)
O(9)-C(29)	1.450(6)	C(9)-O(9)-C(29)	122.1(4)
Mn(1)-C(2, 3)*	1.759(6)	C(1)-C(17)-C(18)	127.1(4)
Mn(2)-(C10, 11)*	1.763(6)	C(9)-C(22)-C(23)	128.2(4)
C(2, 3)-O(2, 3)*	1.170(6)	C(1)-C(17)-C(21)	127.7(4)
C(10, 11)-O(10, 11)*	1.157(7)	C(9)-C(22)-C(26)	127.0(4)
Torsion angles			
C(2)-Mn(1)-C(1)-O(1)		-144.7(4)	
C(10)-Mn(2)-C(9)-O(9)		-50.1(4)	
Mn(1)-C(1)-C(17)-C(18)		-5.0(6)	
Mn(2)-C(9)-C(22)-C(26)		-5.2(6)	
O(1)-C(1)-C(17)-C(21)		4.7(6)	
O(9)-C(9)-C(22)-C(23)		5.1(6)	

*   Averaged value
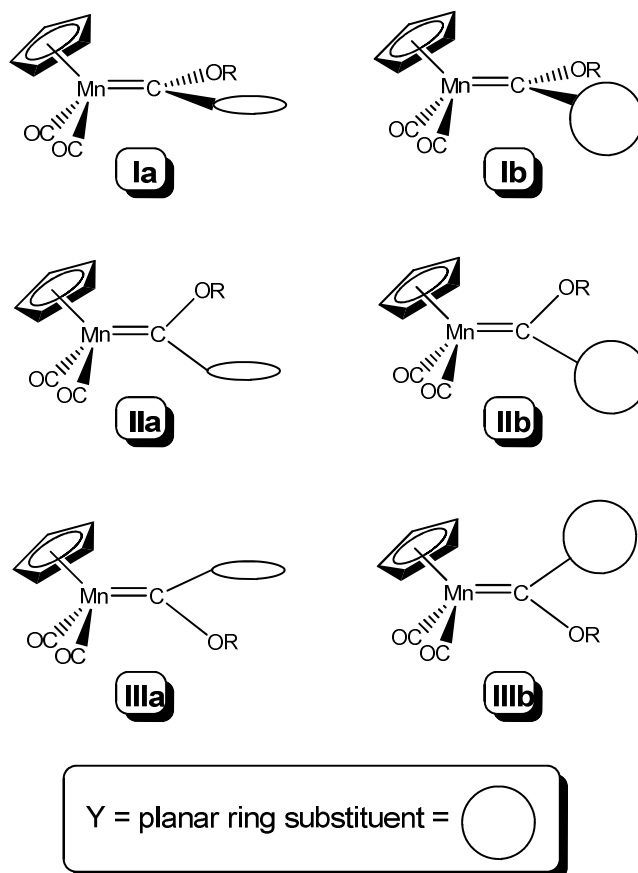
Figure 3.20   Possible conformations/geometric isomers of carbene complexes [MnCp(CO)$_2${C(OR)Y}]

Kostić and Fenske[75] have calculated the relative energies of the isomers/conformations **I** – **III** and found **IIb** to be the most stable where the ring substituent is approximately co-planar to the carbene plane. **I** was found to be the least stable, with a barrier for the rotation of the carbene ligand about the Mn-C(carbene) axis. Comparison of known structures of [MnCp(CO)$_2$(carbene)] complexes[19,20,76] shows that, as predicted by theory, the orientation of the carbene plane approximately in the mirror plane of the MnCp(CO)$_2$-fragment (**II** and **III** in Figure 3.20) is more favourable than the orientation perpendicular to it (conformer **I**).   In the case of complex **23**, however, it was found that the

---

[75] Kostić, N.M.; Fenske, R.F. *Organometallics* **1982**, *1*, 974.

[76] (a) Fischer, E.O.; Kleine, W.; Shambeck, W.; Schubert, U. *Z. Naturforsch., B.: Anorg. Chem. Org. Chem.* **1981**, *36B*, 1575, (b) Friedrich, P.; Besl, G.; Fischer, E.O.; Huttner, G. *J. Organomet. Chem.* **1977**, *139*, C68, (c) Herrmann, W.A.; Weidenhammer, K.; Ziegler, M.L. *Z. Anorg. Allg. Chem.* **1980**, *460*, 200, (d) Fontana, S.; Schubert, U.; Fischer, E.O. *J. Organomet. Chem.* **1978**,*146*, 39.

carbene plane is twisted about 85° relative to the mirror plane, giving it the conformation of **Ia** as illustrated above. This also means that the ring substituent is perpendicular to the carbene plane. Only two other structures exhibit conformation **I** : [MnCp(CO)$_2${C(OMe)menthyl}][76(d)] and [Mn((MeCp)(CO)$_2${C(OMe)PMe$_3$}][20] In all of these complexes, the carbene carbon carries bulky substituents, forcing the carbene plane to orient in a less favourable way with respect to the MnCp(CO)$_2$-fragment. Also in the case of biscarbene complexes[52] was conformation **I** not observed.

MnCp(CO)$_2$-moieties exhibit high backbonding ability and supply sufficient electron density to the carbene carbon so that π-donating organic substituents at the carbene carbon are not essential to stabilize of these types of complexes. A structural consequence of the above statement is the longer C(carbene)-O bond distance (1.340(5) Å) than for Group VI alkoxycarbene complexes in which alkoxy groups serve as π-donating substituents.[19] The ethoxy group poorly competes with the MnCp(CO)$_2$-moiety for π-bonding with the carbene carbon. This is also true for most other [MnCp(CO)$_2$(carbene)] complexes, however, a significantly longer Mn-C(carbene) bond length is found for **23** than for other reported cyclopentadienyl manganese carbene complexes.[19,76] In most cases, the Mn-C(carbene) bond distance was reported as being (1.85-1.87 Å), not significantly influenced by the nature of the organic substituents. For the ferrocenyl-substituted **23**, Mn-C(carbene) distances of 1.924(5) and 1.916(5) Å were observed, thereby the π-donating ability of the ferrocenyl substituent considerably can be inferred as less backdonation of the MnCp(CO)$_2$-fragment is required.

For complexes of the type [Re$_2$(CO)$_9$(carbene)], the favoured electronic position for the carbene ligand is *cis* to the rhenium-rhenium bond. Neutral rhenium carbonyl complexes require one X-type ligand, which is a bulky Re(CO)$_5$-fragment for the complexes **27** and **33**. Thus the carbene ligand should lie in the equatorial plane and be in a staggered conformation with respect to the carbonyl ligands of the equatorial plane of the other Re(CO)$_5$ group. This is true for **27** but not for **33**.
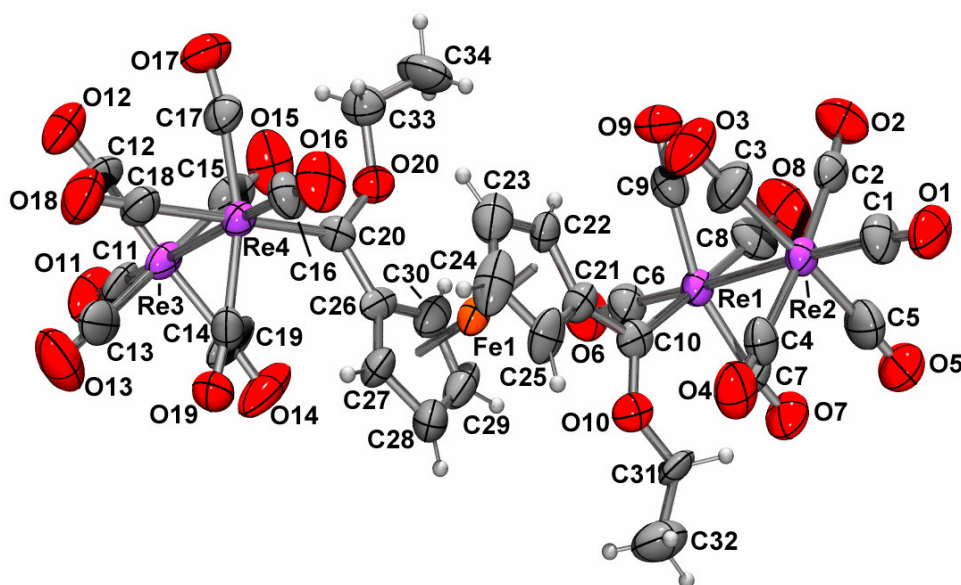
Figure 3.21   ORTEP + POV-Ray drawing of the molecular structure of **27**. Atomic displacement ellipsoids are shown at the 50% probability level.
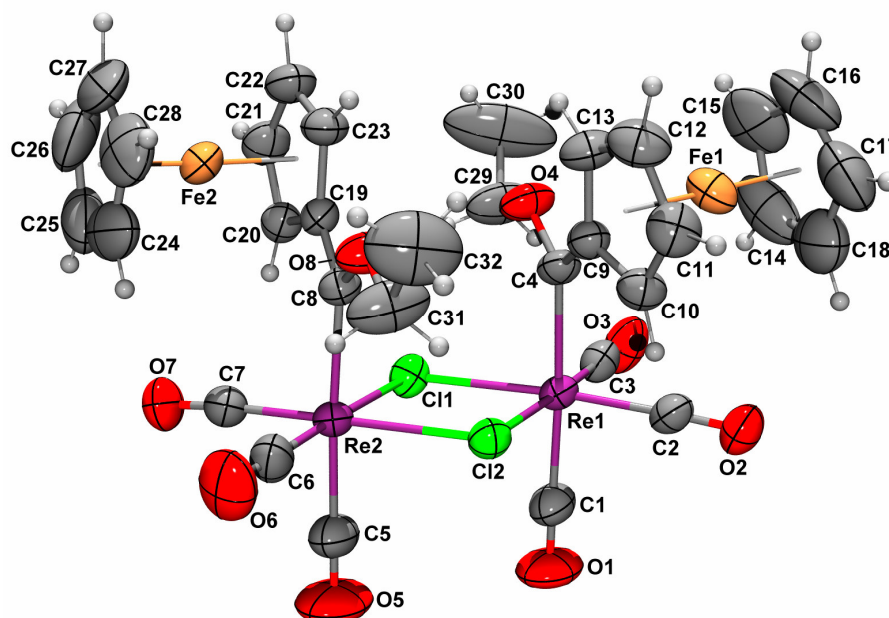
Figure 3.22   ORTEP + POV-Ray drawing of the molecular structure of **28**. Atomic displacement ellipsoids are shown at the 50% probability level.
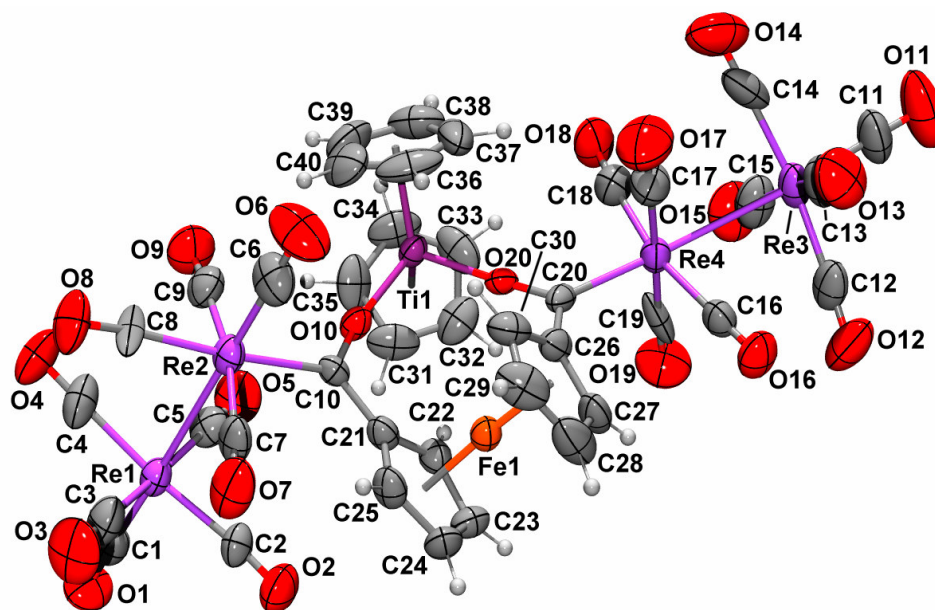
Figure 3.23   ORTEP + POV-Ray drawing of the molecular structure of **33**. Atomic displacement ellipsoids are shown at the 50% probability level.

The geometries of the two rhenium-carbene carbon termini in the biscarbene complexes **27** and **28** are approximately equivalent, but complex **33** is exceptional in that one of the carbene ligands has sacrificed the electronic favoured equatorial position for an axial position. This is one of the rare examples for dirhenium nonacarbonyl complexes to deviate from equatorially coordinated ligands. Fischer and Rustemeyer[27, 28] reported a rhenium octacarbonyl complex containing two carbene ligands and found one of the carbene ligands in an equatorial and the other in an axial position, *eq,ax*-[{Re(CO)$_4${C(OEt)SiPh$_3$}}$_2$].

In **28**, there are only two monorhenium fragments but the orientations are nevertheless retained through the two bridging chloro ligands. The Re-Re distance is *ca*. 0.8 Å longer because of these bridging ligands.

Table 3.18   Selected bond lengths (Å) of ferrocenyl rhenium biscarbene complexes **27**, **28** and **33**

| Bond lengths	**27**	Bond lengths	**28**	Bond lengths	**33**
Re(1)-Re(2)	3.0974(9)	Re(1)---Re(2)	3.9046(4)	Re(1)-Re(2)	3.0712(8)
Re(3)-Re(4)	3.0632(9)			Re(3)-Re(4)	3.0569(8)
Re(2)-C(1)	1.924(19)	Re(2)-C(1)	1.953(7)	Re(1)-C(1)	1.912(17)
Re(3)-C(11)	1.93(2)	Re(2)-C(5)	1.959(8)	Re(3)-C(11)	1.912(18)
Re(1)-C(10)	2.111(15)	Re(1)-C(4)	2.171(6)	Re(2)-C(10)	2.178(11)
Re(4)-C(20)	2.108(14)	Re(2)-C(8)	2.166(6)	Re(4)-C(20)	2.059(13)
C(10)-O(10)	1.355(17)	C(4)-O(4)	1.321(7)	C(10)-O(10)	1.286(14)
C(20)-O(20)	1.327(16)	C(8)-O(8)	1.324(7)	C(20)-O(20)	1.272(14)
C(10)-C(21)	1.460(19)	C(4)-C(9)	1.437(9)	C(10)-C(21)	1.448(17)
C(20)-C(26)	1.493(19)	C(8)-C(19)	1.441(8)	C(20)-C(26)	1.481(18)
O(10)-C(31)	1.449(16)	O(4)-C(29)	1.451(9)	O(10)-Ti(3\1)	1.968(9)
O(20)-C(33)	1.444(18)	O(8)-C(31)	1.457(9)	O(20)-Ti(1)	1.929(8)
Re(1)-C(6,7,8,9)*	1.958(19)	Re(1)-C(2,3)*	1.888(7)	Re(2)-C(6,7,8,9)*	1.949(16)
Re(4)-C(16,17,18,19)*	1.952(18)	Re(2)-C(6,7)*	1.890(8)	Re(4)-C(16,17,18,19)*	1.936(18)
-	-	Re(1)-Cl(1)	2.5252(15)	-	-
		Re(1)-Cl(2)	2.5289(15)		
		Re(2)-Cl(1)	2.5249(15)		
		Re(2)-Cl(2)	2.5351(15)		

*   Averaged value

The rhenium-carbene distances listed above display double bond character with an sp^2-hybridized carbene carbon atom and defines a carbene plane (Re-C-(O(X))-C(Fc)). A second plane is that of the ferrocenyl Cp-rings, and ideally, because of π-conjugation, will be coplanar with the carbene plane. This plane is twisted approximately 16° for **27** (torsion angles Re(1)-C(10)-C(21)-C(25) and Re(4)-C(20)-C(28)-C(30) are -164.0(12) and 163.3(11)°, respectively) due to steric effects (Table 3.19).

Table 3.19 Selected bond angles (°) and torsion angles (°) of ferrocenyl rhenium biscarbene complexes **27**, **28** and **33**

Bond angles	**27**	Bond angles	**28**	Bond angles	**33**
Re(2)-Re(1)-C(10)	84.2(4)	-	-	Re(1)-Re(2)-C(10)	95.0(3)
Re(3)-Re(4)-C(20)	90.7(4)			Re(3)-Re(4)-C(20)	175.1(3)
Re(1)-C(10)-O(10)	129.2(10)	Re(1)-C(4)-O(4)	127.07(4)	Re(2)-C(10)-O(10)	120.6(8)
Re(4)-C(20)-O(20)	128.7(10)	Re(2)-C(8)-O(8)	127.29(4)	Re(4)-C(20)-O(20)	125.7(10)
Re(1)-C(10)-C(21)	125.9(12)	Re(1)-C(4)-C(9)	125.35(5)	Re(2)-C(10)-C(21)	126.4(8)
Re(4)-C(20)-C(26)	126.4(11)	Re(2)-C(8)-C(19)	125.02(5)	Re(4)-C(20)-C(26)	120.6(8)
C(10)-O(10)-C(31)	122.0(12)	C(4)-O(4)-C(29)	123.81(6)	C(10)-O(10)-Ti(1)	161.3(8)
C(20)-O(20)-C(33)	125.5(12)	C(8)-O(8)-C(31)	124.38(6)	C(20)-O(20)-Ti(1)	176.2(8)
C(10)-Re(1)-C(6)	89.0(7)	C(4)-Re(1)-C(3)	93.7(3)	C(10)-Re(2)-C(6)	87.6(5)
C(20)-Re(4)-C(16)	90.1(6)	C(8)-Re(2)-C(7)	93.9(2)	C(20)-Re(4)-C(16)	97.4(5)
C(10)-Re(1)-C(8)	177.1(6)	C(1)-Re(1)-C(4)	175.9(3)	C(10)-Re(2)-C(8)	172.2(8)
C(20)-Re(4)-C(18)	175.3(7)	C(5)-Re(2)-C(8)	176.6(3)		
O(10)-C(10)-C(21)	104.8(13)	O(4)-C(4)-C(9)	107.4(5)	O(10)-C(10)-C(21)	113.0(10)
O(20)-C(20)-C(26)	104.9(12)	O(8)-C(8)-C(19)	107.6(5)	O(20)-C(20)-C(26)	112.8(11)
-	-	Re(1)-Cl(1)-Re(2)	101.28(5)	-	-
		Re(1)-Cl(2)-Re(2)	100.90(5)		
Torsion angles	**27**	Torsion angles	**28**	Torsion angles	**33**
C(6)-Re(1)-C(10)-O(10)	91.6(14)	C(3)-Re(1)-C(4)-O(4)	50.7(6)	C(6)-Re(2)-C(10)-O(10)	103.8(9)
C(16)-Re(4)-C(20)-O(20)	-91.56(1)	C(6)-Re(2)-C(8)-O(8)	45.6(6)	C(16)-Re(4)-C(20)-O(20)	-175.57(1)
Re(1)-C(10)-C(21)-C(22)	17(2)	Re(1)-C(4)-C(9)-C(10)	14.35(1)	Re(2)-C(10)-C(21)-C(22)	156.8(10)
Re(4)-C(20)-C(26)-C(27)	-23(2)	Re(2)-C(8)-C(19)-C(20)	10.2(9)	Re(4)-C(20)-C(26)-C(27)	-56.0(17)
Re(1)-C(10)-C(21)-C(25)	-164.0(12)	Re(1)-C(4)-C(9)-C(13)	-179.23(5)	Re(2)-C(10)-C(21)-C(25)	-21.6(19)
Re(4)-C(20)-C(28)-C(30)	163.3(11)	Re(2)-C(8)-C(19)-C(23)	-179.5(5)	Re(4)-C(20)-C(26)-C(30)	-48.6(17)
Re(1)-C(10)-O(10)-C(31)	-1.36(2)	Re(1)-C(4)-O(4)-C(29)	-10.67(9)	Re(2)-C(10)-O(10)-Ti(1)	121.43(2)
Re(4)-C(20)-O(20)-C(33)	13.72(2)	Re(2)-C(8)-O(8)-C(31)	-6.93(9)	Re(4)-C(20)-O(20)-Ti(1)	-89.54(12)

The longer Re-Re distance observed in **28**, however, allows for the two carbene ligands to lie on the same side of the Re_2Cl_2-plane, with the ethoxy group of one carbene ligand stacked across the Fe-Cp ring of the other, and the ferrocenyl Cp-rings co-planar with the defined carbene plane (Re(1)-C(4)-C(9)-C(19) - 179.2(5)°, Re(2)-C(8)-C(19)-C(23) -179.5(5)). The sterically hindered metallacycle formed by the bridging biscarbene ligand of **33** results in a large twist in the carbene and ferrocenyl planes and the corresponding torsion angles, Re(2)-C(10)-C(21)-C(25) and Re(4)-C(20)-C(26)-C(30), are -21.6(19) and -48.6(17)° respectively.

Table 3.20   Selected bond lengths (Å) and angles (°) around the carbene carbon atoms, specified as equatorial, axial or *cis*-substituted carbenes
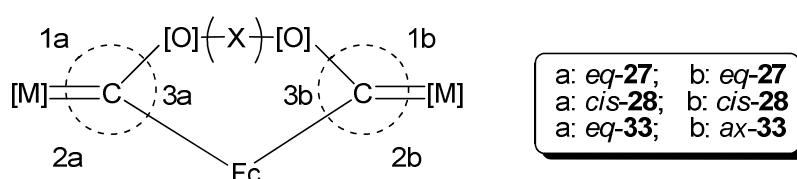
Angle	27		28		33	
	(a: *eq*)	(b: *eq*)	(a: *cis*)	(b: *cis*)	(a: *eq*)	(b: *ax*)
1	129.2(10)	128.7(10)	127.07(4)	127.29(4)	120.6(8)	125.7(10)
2	125.9(12)	126.4(11)	125.35(5)	125.02(5)	126.4(8)	120.6(8)
3	104.8(13)	104.9(12)	107.4(5)	107.6(5)	113.0(10)	112.8(11)
Bond	27		28		33	
	(a: *eq*)	(b: *eq*)	(a: *cis*)	(b: *cis*)	(a: *eq*)	(b: *ax*)
M-C$_{carb}$	2.111(15)	2.108(14)	2.171(6)	2.166(6)	2.178(11)	2.059(13)
C$_{carb}$-O	1.355(17)	1.327(16)	1.321(7)	1.324(7)	1.286(14)	1.272(14)
C$_{carb}$-C(Fc)	1.460(19)	1.493(19)	1.437(9)	1.441(8)	1.448(17)	1.481(18)

The two complexes **27** and **28** both have ethoxy substituents adopting an orientation with their methylene carbon atoms towards the metal carbonyl ligands, which is electronically favoured.[77]

The carbene substituent bond lengths and angles around each carbene carbon atom of the biscarbene ligands are summarized in Table 3.20. Complex **33** has both the longest and the shortest Re-C(carbene) bond lengths. The axial substitution of the one carbene places the ligand *trans* to the $Re(CO)_5$-fragment, where negligible competition for π-backdonation from the Re-atom is expected. A shorter bond length (2.059(13) Å) and higher bond order than the mean value reported for terminal alkoxycarbenes (2.098 Å)[78] is observed. In contrast, a significantly longer equatorial Re-C(carbene) bond distance of 2.178(11) Å corroborates the findings of the previous chapter: the acyl resonance structure contributes predominantly to the carbene complex's structure (Figure 2.29). Even stronger support of this supposition is the fact that for both the equatorial and axial carbene ligands, the C(carbene)-O bond length is found to be 0.035 – 0.08 Å shorter than those of the corresponding ethoxycarbene complexes, irrespective of substitution site, as well as the near linear C(carbene)-O-Ti angles (161.3(8), 176.2(8)°). For the O-C(carbene)-C(ring) bond angle, **33** shows a significantly larger angle for both the equatorial and the axial carbene ligands (113.0(10)° and 112.8(11)°) compared to the smaller angles for **27** and **28** (104.8(13)°, 104.9(12)° and 107.4(5)°, 107.6(5)°, respectively). This observation seems to indicate that the loss in electronic stability of the equatorial position is compensated for by the sterically more favourable axial coordination.

3.4.5.2   Crystal packing

Packing of the manganese and rhenium crystal structures obtained seemed to be mostly governed by closest-packing, although a few interesting features were

---

[77] Fernández, I.; Cossío, F.P.; Arrieta, A.; Lecea, B.; Mancheño, M.J.; Sierra, M.A. *Organometallics* **2004**, *23*, 1065.

[78] Orpen, A.G.; Brammer, L.; Allen, F.H.; Kennard, O.; Watson, D.G.; Taylor, R. *J. Chem. Soc., Dalton Trans.* **1989**, S1.

observed. The Mercury software[79] available from the CCDC[80] was employed to determine the presence of H-bonds or other short-contact bonds in the crystal lattices.

Complex **23** displayed a pattern of metal carbonyl layers, alternated by an 'organic' layer made up of ferrocenyl and ethoxy groups, as shown in Figure 3.24.
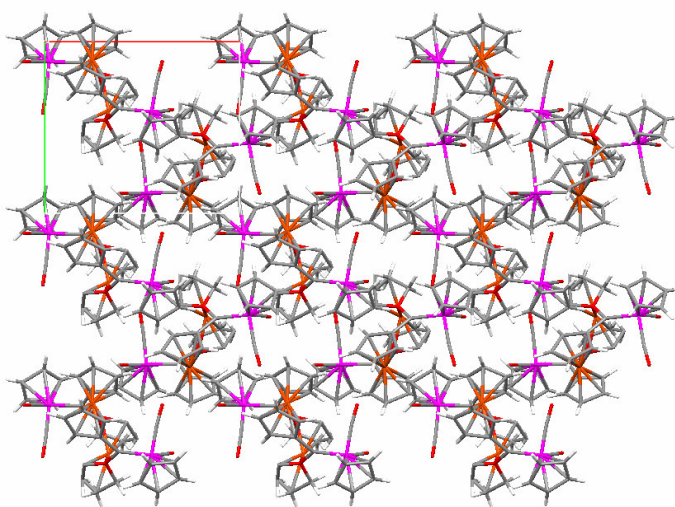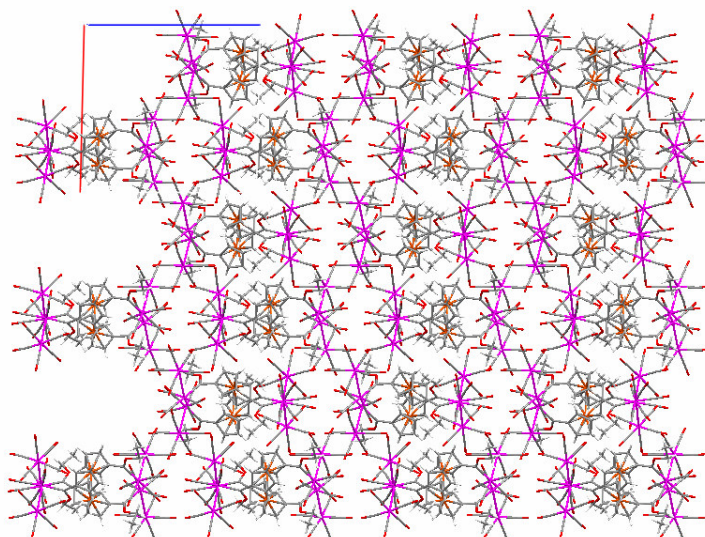

Figure 3.24   View along the *c*-axis of **23**

Complex **27** exhibits another variation of this layered packing, in that the metal carbonyl groups (Figure 3.25) cluster together in a staggered two-layered fashion.

---

[79] (a) Mercury CSD 2.0 - New Features for the Visualization and Investigation of Crystal Structures, Macrae, C.F.; Bruno, I.J.; Chisholm, J.A.; Edgington, P.R.; McCabe, P.; Pidcock, E.; Rodriguez-Monge, L.; Taylor, R.; van de Streek, J.; Wood, P.A. *J. Appl. Cryst.* **2008**, *41*, 466, [DOI: 10.1107/S0021889807067908], (b) Mercury: visualization and analysis of crystal structures, Macrae, C.F.; Edgington, P.R.; McCabe, P.; Pidcock, E.; Shields, G.P.; Taylor, R.; Towler, M.; van de Streek, J. *J. Appl. Cryst.* **2006**, *39*, 453, [DOI: 10.1107/S002188980600731X].
[80] The Cambridge Structural Database: a quarter of a million crystal structures and rising Allen, F.H. *Acta Cryst.* **2002**, *B58*, [DOI: 10.1107/S0108768102003890].
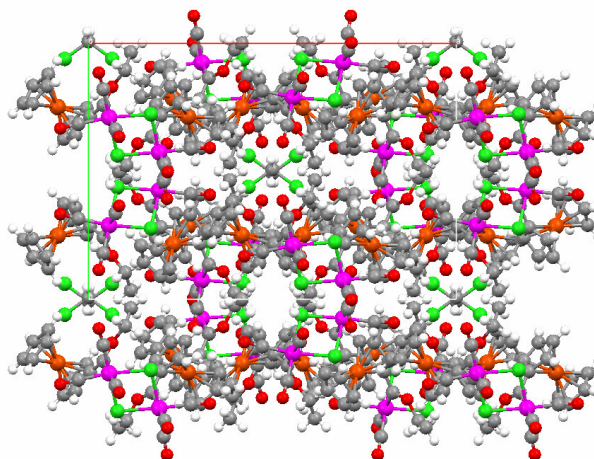
Figure 3.25   View along the *b*-axis of **27**

Layered packing was not observed for the titanoxy analogue **33** of **27**, instead, discrete clusters of the complexes formed channels bordered by the carbonyl-O atoms.
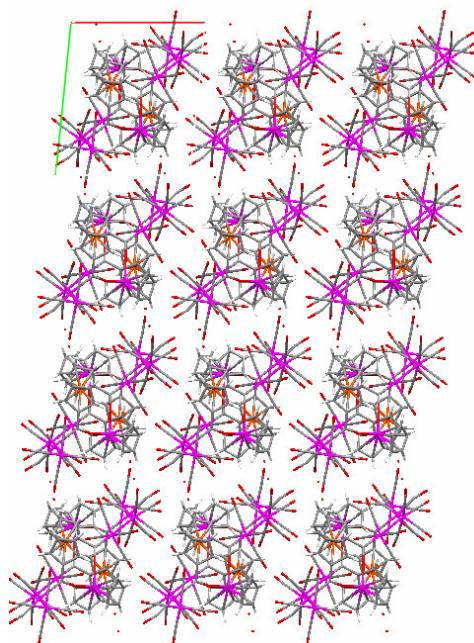
Figure 3.26   View along the *c*-axis of **33**

Figure 3.27   View along the *c*-axis of **28**

In the case of complex **28**, channels filled by inclusion solvent dichloromethane molecules were observed similar to the structure of the ferrocenyl titanoxycarbene complex of chromium (**5**). Besides ordered close-packing, no other inter- or intramolecular forces determining crystal packing could be identified.

3.5   Concluding remarks

Group VII transition metal cluster carbene complexes were synthesized from mononuclear [MnCp(CO)$_3$] and binary dinuclear [Re$_2$(CO)$_{10}$] starting materials. After alkylation with an oxonium salt, the known complex [MnCp(CO)$_2$\{C(OEt)Fc\}] **22** and the novel biscarbene complex **23** [μ-Fe\{C$_5$H$_4$C(OEt)MnCp(CO)$_2$\}$_2$] were isolated. Reaction quenching with titanocene dichloride instead of alkylation lead to the formation of the cluster carbene complexes **24** [MnCp(CO)$_2$\{C(OTiCp$_2$Cl)Fc\}] and the corresponding biscarbene complex **25** [\{μ-TiCp$_2$O$_2$-O,O'\}\{μ-Fe(C$_5$H$_4$)$_2$-C,C'\}[CMnCp(CO)$_2$\}$_2$]. This complex also displays the unique bimetallacyclic bridging carbene ligand as first prepared in Chapter 2.

From the crystal structure of **23** it was seen that the complex displays an unusual conformation, where the carbene plane is approximately perpendicular to the mirror plane of the MnCp(CO)$_2$-fragment, and the ferrocenyl substituent is again perpendicular to the carbene plane. From literature, this conformation is described as the least stable.[75]

After preparation of the monolithiated ferrocene from iodoferrocene, the well known Fischer-method of carbene synthesis was employed to synthesize the monocarbene complex **26** [Re$_2$(CO)$_9${C(OEt)Fc}]. Evidence of both axial and equatorial isomers was seen in the spectroscopic data, but the two isomers could not be separated. This lead to the supposition that an equilibrium exists between the two isomers, as the one conformation is electronically more stable (equatorial) and the other is less sterically hindered (axial isomer).

During the synthesis of the biscarbene complex **27**, *eq,eq*-[μ-Fe{C$_5$H$_4$C(OEt)Re$_2$(CO)$_9$}$_2$], another biscarbene complex was obtained. Complex **28** *fac*-[(μ-Cl)$_2$-(Re(CO)$_3${C(OEt)Fc})$_2$] exhibited a cleaved Re-Re bond, and the proposed reaction mechanism for the complex formation requires abstraction of a chlorine atom from the solvent dichloromethane, the only possible chlorine source. It is anticipated that this compound originated from the tetracarbonyl precursor, [Re(CO)$_4${C(OEt)Fc}Cl].

Dilithiation of ferrocene, followed by subsequent metalation with dirhenium carbonyl and titanocene dichloride yielded the target monocarbene complex **31** *ax*-[Re$_2$(CO)$_9${C(OTiCp$_2$Cl)Fc}] and biscarbene **33** *ax,eq*-[{μ-TiCp$_2$O$_2$-O,O'}{μ-Fe(C$_5$H$_4$)$_2$-C,C'}{CRe$_2$(CO)$_9$}$_2$], both displaying the unusual axial substitution of the carbene ligand (although in the biscarbene complex, one axial and one equatorial ligand was observed). A range of other products was also isolated form the reaction mixture. Products such as [Re(CO)$_5$Cl], [Re$_3$(CO)$_{14}$H] (**29**), [Re(CO)$_5${C(O)Fc}] (**30**), FcCHO and Fc-Fc, [(μ-H)$_2$-(Re(CO)$_4${C(O)Fc})$_2$] (**34**) and *eq*-[Re$_2$(CO)$_9${C(OTiCp$_2$Cl)(Fc'CHO)}] (**32**) were characterized.

Two possible reaction mechanisms for the formation of these products were proposed; one involving proton transfer form solvents *via* a radical mechanism

involving hidrido intermediates such as [Re(CO)$_5$H]. This mechanism is supported by the finding of the dimerization decomposition product diferrocene. The other mechanism involves acyl hydrido intermediates from ionic hydrolysis reaction with trace amounts of water present. Reductive elimination then yields the decomposition product formylferrocene (FcCHO), as well as the FcCHO-substituted carbene ligand in complex **32**. In both cases, the weak Re-Re bond is broken, as shown by the ease of metal-metal bond breaking in the mass spectrometric data.

Complex **34** is the ferrocenyl analogue of the acyl hydrido thienyl hydroxycarbene complexe synthesized previously in our laboratories, showing the same bridging hydride and bridging hydroxyl-acyl ligands as the Shvo catalyst. However, some doubt exists about the existence of the O-H-O bridge in complex **34**, as evidenced by NMR and IR spectroscopy.

NMR spectroscopy was used to determine a trend in π-electron donor strength of the central metal moieties of the complexes synthesized in both Chapter 2 and 3. The donor abilities of the metal fragments could be arranged in increasing order as Re$_2$(CO)$_9$ < W(CO)$_5$ < Cr(CO)$_5$ < Mo(CO)$_5$ < MnCp(CO)$_2$.